Response to divergent selection on meiotic recombination in *Saccharomyces cerevisiae*

Xavier Raffoux[1], Xanita Saayman[2], Walaa A. Abuelgassim[1], Thomas Maret[1], Anthony Venon[1], Fabrice Dumas[1], Lorenzo Tattini[2], Olivier C Martin[3], Gianni Liti[2], and Matthieu Falque[1]

[1] Université Paris-Saclay, INRAE, AgroParisTech, GQE - Le Moulon, 91190 Gif-sur-Yvette, France. [2] Université Côte d'Azur, CNRS, INSERM, IRCAN, 06107 Nice, France. [3] Université Paris-Saclay, CNRS, INRAE, Université Evry, Institute of Plant Sciences Paris-Saclay (IPS2), 91190 Gif-sur-Yvette, France.

Running head:

Divergent Selection on Recombination in Yeast

Corresponding author:

Matthieu Falque

E-mail: matthieu.falque@inrae.fr

Keywords

Meiotic recombination, crossover, interference, divergent selection, yeast

Abstract

Meiotic recombination is a key driver of evolution in sexually reproducing organisms, reshaping genetic diversity by generating novel allelic combinations. The rate of recombination varies substantially across living organisms depending on *cis*- or *trans*-acting genetic elements, as seen in many species, including the yeast *Saccharomyces cerevisiae*. Here, we report on an experimental evolution-based study to better understand the factors shaping this natural variation. Starting with a genetically diverse population of *S. cerevisiae*, we have carried out recurrent divergent selection on recombination rate using a fluorescence-based sorting approach in four independent lineages. After ten generations, we observed an average response of recombination rate of +28% after positive selection and -24% after negative selection, within the interval used for selection. In the adjacent re-

gion, however, we observed a weaker response in the opposite direction, and no response in four other unlinked genomic regions. Whole-genome sequencing of individuals selected for high recombination revealed mixed outcomes in the four independently evolved lineages. All four lineages showed selection for high recombination locally, with particular haplotypes heavily favored and sequence- or structural variation-based heterozygosity selected against within the selection interval. However, only two of the four lineages showed increases in genome-wide recombination rate. Overall, this experimental evolution approach provides original and useful insights into the evolvability of the meiotic recombination rate and the associated genetic determinants.

Introduction

Meiosis is considered one of the major evolutionary innovations of eukaryotes. The associated genetic recombination is at the heart of many evolutionary processes, both under natural selection (Burt and Bell 1987) and in the genetic improvement of domesticated species (Hill and Robertson 1966; Tourrette et al. 2019). Crossovers (COs) occurring during prophase of the first meiotic division have two major consequences: they generate a physical link between homologous chromosomes, which allows a balanced segregation of homologs at anaphase I, required for the viability of the gametes, and they shuffle the parental haplotypes to produce novel allelic combinations in the recombinant gametes. During meiotic prophase I, a large number of programmed DNA double-strand breaks are produced on the chromatids. They are then repaired by several possible pathways which use the homolog as a template — leading to the formation of a minority of COs, which are reciprocal exchanges of genetic material between homologs, and a majority of non-crossovers, which are non-reciprocal short tract exchanges producing gene conversions (GCs), or which use the sister chromatid as a template with no genetic consequence. Two distinct pathways have been demonstrated to exist in many organisms for CO formation (Higgins et al. 2004; Housworth and Stahl 2003; Falque et al. 2009), one of them being sensitive to the phenomenon of interference that reduces the probability of two COs occurring close to each other (Sturtevant 1915), and the other one being insensitive to interference.

CO number and distribution along chromosomes are strongly regulated (Pan et al. 2011). The number of COs per chromosome usually ranges between one and three, and is similar across species, in spite of very large differences in physical chromosome sizes (Fernandes et al. 2017). The

distribution of COs along chromosomes, often referred to as the CO landscape, is usually uneven, e.g. in yeast (Mancera et al. 2008), which is due to a combination of different factors, including interference (Morgan et al. 2024). Large pericentromeric regions are almost void of COs in many organisms (Haenel et al. 2018), and some very small regions can have high densities of COs (hotspots). CO regulation shows several similar features in various species, see review in (Dluzewska et al. 2018). Among them, (1) CO assurance (Jones 1984) ensures that at least one CO occurs per bivalent during meiosis, allowing faithful chromosome segregation, (2) CO homeostasis (Martini et al. 2006) keeps the rate of COs almost constant even if the number of double-strand breaks is reduced, (3) CO interference (Sturtevant 1915; Morgan et al. 2024) leads to COs being more regularly spaced than if they were placed at random, (4) heterochiasmy (Sardell and Kirkpatrick 2020) leads to different levels and landscapes of recombination in male *vs* female meiosis, and (5) natural genetic variation of CO rate distribution is observed within many species (Kong et al. 2010; Bauer et al. 2013; Brekke et al. 2023; Johnston 2024). Finally, the recombination rate (hereafter noted RR) also shows some phenotypic plasticity, for instance as a response to variation in temperature (Lloyd et al. 2018) or nutritional state (Abdullah and Borts 2001; Novak et al. 2026).

There are two types of genetic determinants of CO formation: *cis* DNA sequences that modulate RR locally in their vicinity and thus change the recombination landscape, and some *trans* factors that affect RR genome-wide. Both contribute to the natural variability of RR, and we estimated their respective contributions to 38% and 17% of the variance of RR in *S. cerevisiae* (Raffoux et al. 2018a). *Cis* effects may involve local heterozygosity (Dluzewska et al. 2018). For significant sequence divergence, recombination decreases as heterozygosity increases (Raffoux et al. 2018a), as expected if strong divergence suppresses COs through the mismatch-repair system (Hunter et al. 1996). Recombination QTLs acting in *trans* have also been detected in several species (Pan et al. 2017; Petit et al. 2017; Ziolkowski et al. 2017). Moreover, RR could be increased in Arabidopsis and in a few crop species by knocking out anti-CO genes (e.g. FANCM, FIGL1 or RECQ4), overexpressing pro-CO genes (e.g. HEI10), or changing the ploidy context in Brassicaceae, see review in Blary and Jenczewski (2019).

Although CO formation is highly regulated, the evolutionary pressures behind such regulations remain unclear. There must be at least one CO per bivalent for gametes to be viable, and there seems also to be a soft upper limit to CO number in most species studied (Fernandes et al. 2017), but the underlying selective pressures remain hypothetical. Recombination is strongly associated with the occurrence of sex, so the fitness cost of recombination itself (crossovers) may not always be easily

distinguished from that of sex (segregation) in experimental evolution approaches, as reviewed in Parée and Teotónio (2025). Sex involves spending both time and energy, and has a 'twofold cost' because the females transmit their genes at only half the rate of asexual equivalents (Bell 1982). Recombination may also increase or decrease fitness (Charlesworth and Barton 1996): it can break beneficial allelic combinations built up by selection, producing the 'recombination load' (Otto and Lenormand 2002), e.g. in *D. melanogaster* where decreased recombination led to higher female fecundity (Barton 2010). Too many COs may also be mutagenic (Liu et al. 2017) or could be mechanically deleterious for meiosis, although evidence for this is still lacking. Yet despite these costs, sex and recombination are maintained in the great majority of species, which is referred to as the 'paradox of sex' (Otto and Lenormand 2002). On the other hand, shuffling alleles through recombination can be beneficial for adaptation by increasing the genetic variance (Barton 2010). Experimental evolution of yeast populations revealed that sexual reproduction favored adaptation to a new harsh environment, whereas no effect was observed in a new benign environment (Goddard et al. 2005), and that sex both speeds up adaptation and allows natural selection to more efficiently sort beneficial from deleterious mutations (McDonald et al. 2016). Altogether, the relationship between recombination and fitness is difficult to study because it is mostly indirect: COs do not directly change fitness (except a small number of COs required to keep euploidy through meiosis), but they modify the potential to exploit standing genetic variation to produce new haplotypic combinations, which may be beneficial (or deleterious) for fitness. Finally, CO interference can also be an important player for the adaptive consequences of recombination since it lowers the probability that two close COs bring together three favorable alleles linked in repulsion phase (Otto and Payseur 2019).

RR shows intraspecific diversity, and many adaptive processes have been found to be associated with the evolution of recombination modifier genes in theoretical (Gandon and Otto 2007) as well as empirical (Korol and Iliadi 1994; Aggarwal et al. 2015) studies. Thus, recombination seems to be able to respond to indirect selection, and it should also be possible to change RR by applying direct recurrent artificial selection. However, selecting on RR is challenging because of the difficulty to measure recombination phenotypes. COs may be detected by studying recombination between genetic markers in linkage mapping experiments (Bauer et al. 2013) or by direct cytological observations. In the latter case, one can measure CO positions by visualizing late recombination nodules using electron microscopy (Anderson et al. 2003) or by immunofluorescence using antibodies against different proteins that concentrate as foci at the location of COs (Anderson et al. 1999; Chelysheva et al. 2012). In all cases, these methods are destructive, and they are difficult to bring to a high

throughput as required for experimental evolution.

Nevertheless, direct selection experiments on RR have already been reported a long time ago in Drosophila, based on the segregation of morphological genetic markers. After six generations of positive or negative selection on CO rate in the interval between loci 'dichaète' and 'sepia', no response to selection was first observed (Gowen 1919), but later on, during 30 generations of selection for low CO rate in the interval between 'white eyes' and 'miniature wings' loci, a continuous reduction of RR was observed (Detlefsen and Roberts 1921). In the same paper, eight generations of selection for high RR in the same interval also produced a reduction of recombination, which was interpreted by the authors as a positive response to selection producing many double COs. Several similar experiments have been performed in other genomic regions of Drosophila (Parsons 1958; Chinnici 1971a; Kidwell 1972; Abdullah and Charlesworth 1974; Charlesworth and Charlesworth 1985a), which confirm that recurrent artificial selection for high or low recombination rate most often results in a genetic response. Further studies on the genetic architecture of the response showed that it is polygenic (Chinnici 1971b; Charlesworth and Charlesworth 1985b) and not due to chromosomal rearrangements. In the insect *Tribolium castaneum*, significant response to selection for high RR has also been reported during 10 generations, after which a plateau was reached, and RR was stable for five more generations (Dewees 1975). In the same paper, when selecting for low RR, there was no significant decrease of RR along generations, but the average RR over the 15 generations was significantly lower than the initial value, suggesting a response limited to the first generation. In *Schistocerca gregaria*, the response to selection was significant for low RR but not for high RR, although there was a trend suggesting a weak response in the second case (Shaw 1972). In silkworm, response to selection was obtained for both low and high RR, as cited by Ebinuma and Yoshitake (1981). Apart from insects, a similar experiment has been achieved in Lima bean (Allard 1963), resulting in significant responses to selection for high RR but no response to selection for low RR. In animals and fungi, we did not find any published results on long-term experimental evolution carried out with artificial selection on RR.

Such studies on the evolvability of CO number can provide useful insights on the evolutionary dynamics of recombination modifier genes that can play a crucial role in adaptation from standing variation, particularly in changing environments (Charlesworth 1993). They can also produce evolved populations with diverged recombination rates, which may then be used for experimental evolution with the aim of studying the impact of recombination rate on the dynamics of adaptation after environmental changes. Moreover, such evolved populations may be used later on to detect

signatures of selection by applying sequencing by the 'evolve and resequence' approach (Long et al. 2015), which could point to recombination QTLs and help identify genes or other genomic elements involved in the control of the quantitative variation of CO rate.

Here, we carried out experimental evolution on a yeast population with high standing genetic variation by applying ten cycles of sexual reproduction with recurrent divergent selection of spores based on their recombination status in a region between two fluorescent markers. We observed a response to selection in the interval where selection was applied and a corresponding inverse response in one neighboring interval. Selecting for recombination over eight cycles led to an increase in homozygosity within the selection interval on both the structural and sequence levels. Genome-wide CO analysis further revealed a global increase in CO rate in two of four lineages without impacting the number of non-crossovers. These results collectively suggest that we successfully selected for high-recombination on both the *cis* and *trans* levels in yeast.

Materials and Methods

Biological material

The original SGRP-4X population (Cubillos et al. 2013) was obtained by inter-crossing for 12 generations four representative *S. cerevisiae* founder strains: YPS128 [North American (NA)], DBVPG6044 [West African (WA)], Y12 [Sake (SA)], and DBVPG6765 [Wine/European (WE)].

The bi-fluorescent strain Mat-a SK1-VI_C1Y2 ho::hygMX ura3::kanMX used to cross to the SGRP-4X population was constructed as previously described (Raffoux et al. 2018b). The TDH3prom-yECerulean-natMX construct (above named "C1") is inserted on chromosome VI at position 17462 bp (S288c_reference_genome_R57-1-1). The 100 bp surrounding the insertion locus are: GCACGTGAAAACGGTGAACGTGGTTGTATACCTTCGATACGGATTTGCTT[CONSTRUCT]ACTAATTGAGAGCAAAATTAGTAAGCGAAATGTGAAAATTGGCTTACGAA. The TDH3prom-Venus-NatMX construct (above named "Y2") is inserted on chromosome VI at position 87 305 bp (S288c_reference_genome_R57-1-1). The 100 bp surrounding the insertion locus are: CCCAGAGAGAAAAAAGGAAAAATTTAGCTATGAAACCTCAATAAGCTTTT[CONSTRUCT]TAATACACCAAAGATTCAAGATAAGAGCATAGAACGAACTGTAGAATAGT.

For recombination phenotyping, we also used the three tri-fluorescent tester strains SK1-I_R2C3Y4, SK1-VI_C1Y2R3, and SK1-VI_R3Y4C5 .

Details of constructs, genomic positions, and physical distances between markers for all fluorescent markers used in this work are given in **Suppl Table S1**.

Culture Media and Drugs

Solid SPOR medium was prepared with 0.25 % yeast extract, 0.1 % glucose, 1 % potassium acetate, and 20 g/L BD Bacto Agar (BD-214030). Nourseothricin was used at a final concentration of 30 mg/L, G418 at 100 mg/L, chloramphenicol at 50 µg/mL, and hygromycin B at 200 µg/mL.

Crossing the SGRP population with SK1-VI_C1Y2

To produce the initial population (G0) of our evolution experiment, we crossed spores from the SGRP-4X population with haploid vegetative cells of the SK1-VI_C1Y2 bi-fluorescent strain.

First, a vegetative liquid culture of the SGRP-4X population was grown overnight (15 mL YPD in 50 mL tubes, 30° C, 200 rpm), then centrifuged 2 min at 2000 rpm. The supernatant was discarded, and cells were resuspended in 800 µL ddH_2O. Then 150 µL was spread on 4 Petri dishes with solid SPOR medium and incubated at 30° C. After ten days of sporulation, cells were picked up from the lawn by scraping one quarter of the Petri dish surface with a bent pipette tip, and resuspended in a 1.5 mL Eppendorf tube containing 750 µL ddH_2O with 5 mg/mL 20T zymolyase (Euromedex, Souffelweyersheim, France) and 100 µL glass beads (0.5 mm diameter, Dutscher 67172 Brumath Ref 1606106). To disrupt tetrads, the tubes were vortexed for 30 sec three times, separated by 30 min incubations at 30° C, then centrifuged for 1 min at 13000 rpm, and the pellets were resuspended by vortexing for 2 min in 200 µL ddH_2O. The suspension, containing mostly vegetative cells, was discarded. Spores, which adhere to the tube plastic, were stripped by adding 600 µL ddH_2O with 0.01% NONIDET NP40 (Sigma-Aldrich, Saint Quentin Fallavier, France) and vortexing 2 min, as described in (Rockmill et al. 1991).

Then, vegetative cells of the haploid Mat-a bi-fluorescent strain SK1-VI_C1Y2 were grown overnight (15 mL YPD liquid culture in a 50 mL tube, 30° C, 200 rpm), centrifuged for 2 min at 2000 rpm, and the pellets were resuspended in 600 µL ddH_2O. These vegetative cells and the spores from the SGRP-4X population were crossed: both cell suspensions were mixed, vortexed for 30 sec, and centrifuged for 2 min at 2000 rpm. Pellets were resuspended in 250 µL ddH_2O, and 200 µL were spread on solid YPD Petri dishes and grown overnight at 30 °C. To select only diploids resulting from the desired cross, each of the four quarters of the Petri dish surface was then scraped and resuspended in 250 µL ddH_2O, and 200 µL was spread on SD medium without uracil and containing nourseothricin. This allowed us to select only diploids originating from crosses between a

SGRP-4X spore (Ura+) and a tester cell (natMX), and none of the three other possible diploid genotypes, nor the remaining parental vegetative cells (**Suppl Figure S1**). Selected diploids were stored and used as the generation zero (G0) to start the selection experiments.

Selection of spores depending on their fluorescence status

Isolated spores from the G0 vegetative population were obtained with the same protocol as presented above. The spore suspension was then analyzed with a MoFlo ASTRIOS Fluorescence-Activated Cell Sorter (FACS; Beckman-Coulter, Villepinte, France) and the associated software Summit for manual investigations, or with the CAYSS R package (Raffoux and Falque 2024) for routine analyses. We first selected events corresponding to the size of spores using a gate in the SSC-Height-Log *vs* FSC-Height-Log graph, then we discarded events containing more than one cell using a gate in the SSC-Height-Log *vs* SSC-Area-Log graph, see more details in Raffoux et al. (2018b). Finally, we analyzed the fluorescence intensity of each spore in yECerulean and Venus channels (excitation at 405 and 488 nm, respectively, emission at 448/59 and 526/52 nm, respectively).

Spores were then selected depending on their fluorescence status and sorted in a Petri dish containing solid YPD with chloramphenicol and glass beads (3 mm diameter). At the end of each sorting, Petri dishes were gently shaken to spread glass beads and cells on the surface of the medium. Fluorescence intensity classes for spore selection were chosen depending on the direction of the selective pressure to be applied: selection of spores recombinant between the fluorescent markers (Sel+; **Figure 1A**), selection of spores non-recombinant between the markers (Sel-; **Figure 1B**), or selection of all events identified as spores, regardless of their recombination status between the markers (Sel=; **Figure 1C**).

In the following, we will represent the phenotype of the two fluorescent markers C and Y by "[MN]" where M is "C" if the marker yECerulean is present or "+" if it is not present, and N is "Y" if the marker Venus is present, and "+" if it is not present. So in even generations of Sel+ experiments, 150,000 [C+] recombinant spores and 150,000 [+Y] recombinant spores were selected (left side of **Figure 1A**), in odd generations of Sel+ experiments, 150,000 [++] recombinant spores and 150,000 [CY] recombinant spores were selected (right side of **Figure 1A**), in Sel- experiments, 150,000 [CY] non-recombinant spores and 150,000 [++] non-recombinant spores were selected (**Figure 1B**), and in Sel= experiments, we sorted a total of 300,000 cells from the four fluorescence classes [CY], [++], [C+], [+Y] (**Figure 1C**), ensuring to sort equal numbers of [CY] and [++] spores, and equal numbers of [C+] and [+Y] spores. Using these procedures for each of the three se-

lection modes (Sel+, Sel-, Sel=), we sorted four biological replicates (noted A, B, C, D) from the initial G0 population, leading to 12 independently evolved populations for each generation, hereafter noted Gn Sel+ A, Gn Sel+ B, Gn Sel+ C, Gn Sel+ D, Gn Sel- A, Gn Sel- B, Gn Sel- C, Gn Sel- D, Gn Sel= A, Gn Sel= B, Gn Sel= C, Gn Sel= D, where *n* is the index of the generation.

After 2 days of incubation at 30 °C, a quarter of the surface of Petri dishes containing each G1 population was scraped using a bent tip, resuspended in 250 µL ddH_2O, vortexed, and spread on Petri dishes containing SPOR medium with chloramphenicol. A second quarter of each Petri dish was also scraped, resuspended in 400 µL liquid YPD and 180 µL 50 % glycerol, vortexed, and stored at -80 °C. After 10 days of incubation at 30 °C, a quarter of each SPOR Petri dish was scraped, and we prepared isolated spores as described above, thus completing the first selection cycle.

This recurrent selection was conducted using the same procedure during 10 generations (noted G1 to G10). Note that as seen before, in the case of Sel+ experiments, fluorescence classes to be selected for recombinant and non-recombinant spores are not the same for even or odd generations.

Furthermore, after the first generation, we observed that Venus fluorescence could exhibit three levels of intensity in spores (Raffoux and Falque 2024), depending on the fluorescent marker gene being present or absent in the spore genome, but also depending on the fluorescent protein being present or absent in the cytoplasm of the mother diploid cell. As an example, in Sel- experiments, some [++] spores can descend from a [++/++] diploid vegetative cell and exhibit the lowest Venus fluorescence intensity (only due to autofluorescence), but other [++] spores can also descend from a [C+/Y+] hemizygous diploid vegetative cell and thus exhibit the intermediate fluorescence intensity due to residual cytoplasmic Venus proteins. The highest fluorescence intensity class corresponds to [CY] or [+Y] spores, which do express the Venus protein. In our selection process, we discarded non-fluorescent spores descending from non-fluorescent diploid mother cells because the recombination status of such spores cannot be determined.

Pool-phenotyping recombination in populations

To phenotype recombination at each generation and for each of the 12 populations (replicates A, B, C, D of selection modes Sel+, Sel-, Sel=), 50,000 non-fluorescent spores were sorted in three different Petri dishes containing 100 µL of vegetative cell suspension (at plateau phase) of each of the three haploid tester strains SK1-I_R2C3Y4, SK1-VI_C1Y2R3, and SK1-VI_R3Y4C5 (**Suppl Figure S2)** .

As the Venus (Y) fluorescent marker can exhibit 3 fluorescence levels as mentioned above, depending on the selection mode, the positions of the gates used to select the non-fluorescent [++] spores to be crossed with the testers were not always the same: In the case of Sel- (**Figure 1B**) and Sel= (**Figure 1C**) experiments, as well as even generations of Sel+ experiments (lower part of **Figure 1A**), we sorted [++] spores belonging to the lowest intensity class of Venus fluorescence. Indeed, these spores were formed by non-fluorescent [++/++] diploids, so the fact that they may or may not have a CO between the marker loci does not affect their probability of being picked up. In the case of odd generations of Sel+ experiments (upper part of **Figure 1A**), all spores come from a diploid hemizygous or homozygous for the presence of the markers, so the Venus intensity levels showed only two peaks, and we had no other choice but to sort [++] spores descending from fluorescent diploids. As shown in the top of **Figure 1A**, half of these diploids are hemizygous for both markers [C+/Y+], so [++] spores descending from these diploids must have recombined between the markers. The other diploids, which are homozygous for the presence of one marker and homozygous for the absence of the other marker, cannot produce [++] spores.

As a consequence, recombination values are comparable only between odd generations or between even generations of Sel+ experiments, but values measured at an odd generation of Sel+ may not be compared to values measured at an even generation. On the other hand, recombination values phenotyped in Sel-, Sel=, and even generations of Sel+ experiments are comparable to each other. Moreover, in odd Sel+ generations (top of **Figure 1A**), non-fluorescent spores must be produced *via* recombination happening in the marker interval during sporulation, whereas in even generations of Sel+ (G0 and bottom of **Figure 1A**) as well as in all generations of Sel- (**Figure 1B**) and Sel= (**Figure 1C**), non-fluorescent spores can also be produced without recombination. So in odd Sel+ generations, an extra selection for high recombination is applied during the phenotyping process, whereas this does not happen in other cases.

After 2 days incubation at 30 °C, a quarter of each Petri dish was scraped and resuspended in a well of a 96-wells plate containing 500 µL ddH_2O. We then applied to these cell suspensions two consecutive 1/8 dilutions by adding 700 µL ddH_2O and transferring 100 µL to a new plate. 50 µL of these diluted cell suspensions were then deposited on Petri dishes (9 patches per Petri dish) containing solid SPOR medium with hygromycin.

After ten days incubation at 30 °C, cells were picked up from the lawn by scraping patches with a bent pipette tip, and suspended in a rack of 96 tubes (Macherey-Nagel Ref 740637) containing 375 µL ddH_2O with 5 mg/mL 20T zymolyase (Euromedex, Souffelweyersheim, France) and

100 µL glass beads (0.5 mm diameter, Dutscher 67172 Brumath Ref 1606106). To disrupt tetrads, the plates were incubated 1 hour at 30 °C and shaken three times for 1 min at 30-minute intervals at a frequency of 23 Hz in a TissueLyser (Qiagen), then centrifuged for 5 min at 4500 rpm. Supernatants were discarded by pipetting, and the pellets were resuspended by shaking as previously in 200 µL ddH_2O. The suspension, mostly containing vegetative cells, was discarded. Spores, which adhere to the tube plastic, were stripped by vortexing 2 min (23 Hz) the tubes containing 400 µL ddH_2O with 0.01 % NONIDET NP40 (Sigma-Aldrich, Saint Quentin Fallavier, France) following Rockmill et al. (1991). The spore suspensions were then analyzed with a CytoFLEX flow cytometer, the associated software CytExpert (Beckman-Coulter, Villepinte, France) for manual analyses, and the dedicated R package CAYSS (Raffoux and Falque 2024), which computes recombination rates in the intervals between markers, and the coefficient of coincidence (CoC) based on the two intervals delimited by the three fluorescent markers in each tester strain. CoC is calculated as the ratio between the observed frequency of double COs (one in each interval) and the expected frequency of such double COs in the absence of interference, the latter being estimated as the product of RRs of both intervals (i.e., assuming CO events are independent of each other). So CoC equals one in the absence of interference, and is below one in case of positive CO interference.

Phenotyping recombination of isolated individuals from G8

Glycerol stocks of the G8 populations were spread on solid YPD Petri dishes with chloramphenicol and incubated for 24 h at 30 °C. Then one quarter was scraped, resuspended in YPD with Glycerol, and stored at -80 °C. Another quarter was scraped in 600 µL ddH_2O, and bi-fluorescent [CY] vegetative cells were sorted by FACS using a MoFlo ASTRIOS (Beckman-Coulter, Villepinte, France). During cell sorting, single bi-fluorescent cells were dropped in each well of three 96-well plates on 100 µL solid YPD. For each of the 12 populations, 288 single cells were sorted. The plates were then incubated for 48 hours at 30 °C.

Ninety-six colonies were picked for each of the four biological replicates of the Sel= populations, and 192 colonies for each of the four biological replicates of the Sel− and Sel+ populations. Each colony was then resuspended in a 96-well plate containing liquid YPD with chloramphenicol and incubated overnight without agitation at 30 °C. Plates were then centrifuged for 6 min at 4500 rpm, supernatant discarded by pipetting, and cells resuspended by adding 50 µL ddH_2O. Then, (1) patches of 10 µL cell suspension were deposited on the surface of a solid rectangular Petri dish containing solid SPOR medium with chloramphenicol and after 30 min drying, plates were incubated 10 days at 30 °C for sporulation, and (2) 150 µL of liquid YPD with glycerol was distributed in the

remaining 40 µL of cells suspension, mixed by pipetting, and stored at -80 °C. After sporulation, cells were picked up from the lawn by scraping patches with a bent pipette tip and suspended in a rack of 96 tubes (Macherey-Nagel Ref 740637) containing 100 µL of ddH_2O with 5 mg/mL 20T zymolyase (Euromedex, Souffelweyersheim, France). To disrupt tetrads, plates were incubated for 1 h at 30 °C, and shaken three times for 1 min at 23 Hz in a TissueLyser (Qiagen) separated by 30 min incubations at 30 °C, and finally centrifuged 5 min at 4500 rpm. Supernatants were discarded by flipping the plate over, and 100 µL glass beads (0.5 mm diameter, Dutscher 67172 Brumath Ref 1606106) were added, as well as 150 µL ddH_2O with 0.01 % NONIDET NP40 (Sigma-Aldrich, Saint Quentin Fallavier, France). Plates were then vortexed 2 min (freq=23Hz) and stored at 4 °C before FACS analysis. Finally, the spore suspensions were analyzed, as for the pool-phenotyping, *via* a CytoFLEX flow cytometer, the associated software CytExpert, and the dedicated R package CAYSS (Raffoux and Falque 2024).

Out of 1,920 isolated diploid cells, (768 Sel+, 768 Sel− , 384 Sel=), 267 strains produced fewer than 2,000 spores (117 Sel+, 109 Sel− , 41 Sel=) and were discarded, as well as 571 which produced spores with a single fluorescence intensity peak (no segregation, due to homozygous marker) for one or both markers (217 Sel+, 175 Sel−, 179 Sel=). These observed frequencies of strains with non-segregating markers were compatible (based on exact binomial test) with the expected values (0.33 for Sel+, 0.33 for Sel− , 0.55 for Sel=; see **Suppl Figure S3**) in the case of Sel+ (observed freq=0.33, *p*-value=0.87) and Sel= strains (observed freq=0.52, *p*-value=0.30), but not for Sel- strains (observed freq=0.26, *p*-value=0.0004).

We then checked single-locus Mendelian segregation in the 1,082 remaining strains (434 Sel+ , 484 Sel−, 164 Sel=) by comparing the allele frequencies F_C and F_Y of C and Y markers in spores with their expected value of 0.5. Allele frequency thresholds were defined as $Thr = median(X_i) \pm 3.MAD(X_i)$, where MAD refers to the Median Absolute Deviation, $MAD = median(|X_i - median(X)|)$. Using these thresholds, 204 strains (90 Sel+, 82 Sel−, 32 Sel=) were outliers because of non-Mendelian segregation for marker C and 206 (93 Sel+, 80 Sel−, 33 Sel=) for marker Y, so a total of 224 strains (98 Sel+, 88 Sel-, 38 Sel=) were discarded (**Suppl Figure S4**).

We also checked for two-loci Mendelian markers segregation in the 858 remaining strains (336 Sel+, 396 Sel−, 126 Sel=) by comparing the genotype frequency ratios $F_{[CY]}/(F_{[CY]}+F_{[++]})$ and $F_{[C+]}/(F_{[C+]}+F_{[+Y]})$ in spores with their expected value of 0.5. Using the same MAD-based genotype

frequency thresholds as above, 35 strains (9 Sel+, 2 Sel−, 24 Sel=) were outliers because of non-Mendelian segregation for genotypes CY *vs* ++, and 22 strains (4 Sel+, 17 Sel−,1 Sel=) for genotypes C+ *vs* +Y, so a total of 57 strains (13 Sel+, 19 Sel-, 25 Sel=) were discarded. We observed a surplus of strains producing an excess of CY and C+ spores (**Suppl Figure S5**) as compared to other categories of non-Mendelian outliers, and that $F_{[CY]}/\left(F_{[CY]}+F_{[++]}\right)$ ratio was higher in Sel= than in the two other modes of selection (**Suppl Figure S6**).

FACS-sorted [CY] vegetative diploid cells from G8 Sel= populations can carry two possible marker haplotypes: CY/++ or C+/+Y, each with a probability of 0.5 (**Suppl Figure S3**). As the cytometry analysis software was parameterized to compute RRs with CY/++ marker configurations, we measured in Sel= strains 44 RR values greater than 0.5 corresponding to C+/+Y configurations and 57 values lower than 0.5, corresponding to CY/++ configurations. This proportion of 0.44 was not significantly different from the expected value of 0.5 (exact binomial test, *p*-value = 0.23).

However, we also obtained RR values greater than 0.5 for 28 Sel+ strains and for one Sel- strain, which does not match with usual genetic expectations (**Suppl Figure S3**). Moreover, two Sel+ strains produced RR values very close to 0.5 (0.488 and 0.491). These 31 strains were discarded from the analysis, and the one with RR=0.491 was selected for whole-genome sequencing (see below).

Tetrad dissection and whole-genome sequencing

Individual strains isolated from Sel+ G8 populations and phenotyped (as described above) were then chosen for tetrad sequencing. Overall, we selected Sel+ individuals with the lowest RR (hereafter denoted [low]) and Sel+ individuals with the highest RR (hereafter denoted [high], see **Suppl Table S2**) of each biological replicate.

Each individual strain was inoculated overnight in 10 ml YPD at 30 °C, shaking at 220 rpm. The following day, overnight cultures were centrifuged, washed in 10 ml ddH_2O, and resuspended in 2 % KAc at ~1 OD_{600}/ml, and left shaking at 23 °C. After one week, samples that were sporulated were tetrad dissected using standard procedures (see below). Of the 16 individual samples, 2 did not sporulate (one from biological replicates A [high] and one from biological replicates C [low]).

For tetrad dissections: 400 µL of the culture was removed and centrifuged (1,000 g, 2 min). Pellets were resuspended in 100 µL dissection buffer (1 M sorbitol, 0.2 mM EDTA, 10 mM sodium phosphate) containing 5 µL zymolyase (UZ1000-A, 5 mg/mL), and incubated for 20 minutes at 37 °C. An additional 400 µL of dissection buffer was added, and samples were placed on ice. After

cooling down, 20 µL was used to perform tetrad dissections with the Singer Tetrad Dissection microscope. Plates were grown at 30 °C for 2 days.

A total of 80 segregants from 20 tetrads (9 from [high] strains, 11 from [low] strains) were chosen for whole-genome sequencing. DNA was extracted using the MegaPure kit (MPY80200) using an overnight culture in 5 ml YPD (shaking at 220 rpm, 37 °C) and submitted for whole-genome microbial sequencing with Novogene.

The sequenced tetrads are named according to the sample from which they were taken. For example, “high_A_2.1” refers to the first tetrad dissection of the second sample of the high-recombination lineages ([high]) sorted from Sel+, of biological replicate A. Tetrads that independently went through meiosis but started from the same isogenic sample can be identified by the final number, e.g., high_A_2.1 and high_A_2.2.

Recombination analysis from tetrad whole-genome sequencing

To reconstruct segregant genotype compositions, diagnostic polymorphisms were identified by first running whole-genome alignment of subtelomere-masked genomes of all four parental genomes, as well as SK1, using progressiveMauve (released 2015-02-13, default parameters) and then extracting polymorphisms unique to each parent. At this point, WA and SK1 unique polymorphisms were merged into one, as they are genetically highly similar. Short read sequences of each segregant were then mapped to the SGD reference genome (S288C, SGD-R64-1-1) using bwa mem (v.0.7.17-r1198-dirty, default parameters) and variants (skipping indels) were called using bcftools (v.1.20). Variants were then cross-referenced with diagnostic parental polymorphisms to identify regions of the genome that could only belong to a single parental genotype (custom scripts, python v.3.12.4). Contiguous tracts belonging to a single parental genotype were then merged, and transition points between genotypes were further refined. To refine transition points: once two adjacent genotypes were known, a second round of identifying diagnostic polymorphisms between the two adjacent genotypes was performed, followed by cross-referencing with segregant variants. Transition points were then called as the base pair directly following the last known unique polymorphism.

To identify structural homology between SK1 and the four parental genomes within the chromosome VI selection interval, mVista (LAGAN, RankVISTA probability threshold $p = 0.5$) was used to determine conserved regions (CNS) between each pair of genomes. We further filtered conserved regions to require a minimum conservation of 85 % and a minimum region size of 1 kbp, and these were visualized using Python.

CO counts were performed manually using genotype patterns, and GC counts were calculated as the number of contiguous blocks that had at least 2 genotypes present but were not 2:2 between chromatids, as quantified using bedtools (v.2.31.1). To adjust for the presence of regions that are genetically identical between all chromatids (which prevents the detection of COs and GCs), the number, size and location of these blocks were identified for each tetrad using bedtools (v.2.31.1). CO counts were adjusted for any genetically identical blocks on chromosome termini, since CO events within internal genetically identical blocks can be partially inferred by surrounding genotypes. GC counts, on the other hand, were adjusted for all genetically identical blocks.

Whole-genome sequencing of an isolated diploid strain with an outlier RR value

We used Oxford Nanopore Technologies to whole-genome sequence one diploid strain (1A-E8) isolated from the G8 Sel+ population, which had a RR of 0.491 classifying it as an outlier.

The high molecular weight DNA extraction was performed based on the protocol of Oxford Nanopore Technologies for yeast DNA, derived from a pre-existing protocol (Denis et al. 2018). The yeast strain was grown overnight in YPD at 30 °C, diluted to OD600 = 0.2 in fresh YPD, and cultured to OD600 ≥ 0.7. Cells were harvested by centrifugation, washed in PBS 1X, and stored at −80 °C. Pellets were resuspended in sorbitol 1 M, treated with zymolyase (1000 U/mL) for 1 h at 30 °C, and centrifuged. A lysis buffer (TrisHCl 114 mM, EDTA 115 mM, NaCl 571 mM, 1.14 % PVP40) was added, followed by SDS 10 % and RNase A, and samples were incubated for 1 h at 50°C. After the addition of TE 1X and potassium acetate 5 M, lysates were clarified by centrifugation. DNA was precipitated with isopropanol, washed with cold 70 % ethanol, air-dried, and resuspended in TE 1X overnight, then stored at −20 °C.

For high-molecular-weight DNA size selection, following a protocol modified from Jones et al. (2021), the samples (3–10 µg) were diluted in TE and mixed 1:1 with 2× Size Selection Buffer (2.5 % PVP-360k, 1.2 M NaCl, 20 mM Tris-Hcl, pH 8). Samples were centrifuged at 10 000 g for 30 min, and the supernatant was discarded. The DNA pellet was washed twice with 70 % ethanol, recentrifuged at 10 000 g for 3 minutes, air-dried, and resuspended in 50 µL TE 1X at 37–50 °C with gentle mixing. DNA quantity was verified using the Qubit dsDNA BR assay (Invitrogen™, Thermo Fisher Scientific).

After quantification, 1 µg of high molecular weight genomic DNA was sequenced using a Ligation Sequencing Kit (Ligation sequencing DNA V14, SQK-LSK114, 2024, Oxford Nanopore Technologies) and a MinION Flow Cell (FLO-MIN114, 2024, Oxford Nanopore Technologies). The library preparation and the sequencing were performed according to the manufacturer’s instructions.

The basecalling was done using Guppy software (one strand basecalling, 7.3.9+b2176f600, 2024, Oxford Nanopore Technologies).

After that, FASTQ files were concatenated and used to build a BLAST database using makeblastdb. Coding sequences of the two fluorescent markers were used as a query to blastn against this database. The makeblastdb and blastn programs used were both from the BLAST+ suite from NCBI (Camacho et al. 2009). For the yECerulean fluorescent marker, the six best BLAST hits were selected with thresholds of ≥ 99 % identity and ≥ 95 % query coverage, whereas for the Venus fluorescent marker, the five best hits were selected with ≥ 97 % identity and ≥ 95 % query coverage. ONT reads corresponding to these selected hits were subsequently blasted against the SK1 genome using the same BLAST+ applications.

Finally, the whole sequence between the two fluorescent markers in the SK1 tester strain (85 kbp) was extracted and blasted against the database built with the ONT reads. The eight best hits were selected with ≥ 99.3 % identity and ≥ 99 % query coverage. ONT reads corresponding to these selected hits were aligned against the chromosome VI of SK1 using BioEdit v7.7.1.0.

For comparative analysis, we extracted the sequences between the positions where the two fluorescent markers were inserted, from the four other founder parents of our population: WA (85 kb), WE (64 kb), SA (66 kb), and NA (86 kb), and blasted these sequences against the database made with our ONT reads. The selection thresholds were ≥ 95 % identity and ≥ 65 % query coverage. This yielded five best hits for WA, four best hits for WE, and three best hits for SA; and using a ≥ 60 % query coverage, three best hits for NA.

Checking for possible effects of fluorescent markers on fitness

To assess the extent to which the presence and/or expression of fluorescent marker genes had an effect on cell fitness, G0 cells were sporulated and spores were isolated from vegetative cells as described above. Then, a total of 2,000,000 spores were sorted by FACS (see below) based on their fluorescence status: non-fluorescent [++], yECerulean only [C+], Venus only [+Y], or with both markers [CY]. Sorted spores from each category were plated on solid YPD supplemented with 50 mg/L chloramphenicol and incubated at 30 °C for 48 h to allow germination and random mating. Diploid cells were then selected in SD medium lacking uracil and lysine. After overnight growth (10 mL SD–ura–lys in 50 mL tubes, 30 °C, 220 rpm), cultures were centrifuged for 5 min at 3 000 rpm, the supernatant was removed, and cells were resuspended in 1 mL ddH_2O. Fitness measurements were then carried out on these diploids by measuring growth rate, sporulation efficiency, and spore viability as explained as follows:

Vegetative growth kinetics were monitored in 200 µL of cell suspension diluted to an OD_{600} of 0.01 and distributed across the wells of a 96-well microplate to account for possible temperature variation within the plate. The remaining wells were supplemented with sterile YPD as negative controls to control potential contamination. In total, five microplates were prepared. Additionally, 300 µL of each suspension was spread onto four SPOR plates, incubated at 30 °C for ten days for subsequent sporulation analysis. Growth kinetics were studied by measuring turbidity every 10 min for 48 h using five custom MiniRead 96-well plate readers (Falque et al. 2024). Growth rates were then computed from the growth curves as the maximum growth rate, using the MiniRead R package and calibration procedures associated with the devices.

Sporulation rates were measured after 10 days of sporulation as before, by quantifying the proportions of tetrads and vegetative cells under the microscope, after scraping cells from the solid medium and resuspending them in 10 µL ddH_2O on a microscope slide.

Spore viability was assessed by sorting single spores by FACS after sporulation of diploids and spore isolation (see before). A total of 768 spores from sporulated G0 diploid cells were sorted and deposited on solid YPD in eight one-well rectangular plates (96 spores per plate) for each spore category. Plates were then incubated at 30 °C for 2 days and colonies were counted.

Fitness assessments of evolved populations at generation eight (G8)

To assess fitness in evolved populations, growth kinetics, sporulation rate, and spore viability were measured as explained before for G0, but from diploid G8 cells coming from each of the three selection modes (Sel+, Sel-, Sel=). For spore viability assessment, a total of 2304 [++] non-fluorescent spores (to limit confounding effects) were sorted from spore preparations of sporulated G8 diploid cells for each of the three selection modes (Sel+, Sel-, Sel=) and deposited onto 24 rectangular YPD plates (96 spores per plate). FACS sorting parameters were set to select spores and discard vegetative cells and debris based on FSC/SSC. Sorted spores from each category (Sel+, Sel-, Sel=) were plated on solid YPD supplemented with 50 mg/L chloramphenicol and incubated at 30 °C for 48 h to allow germination and random mating. Fitness measurements were then carried out on these diploids by measuring growth rate, sporulation efficiency, and spore viability as described before.

Statistical analyses

All data analyses and statistical tests were carried out using R v4.5.0 or python v.3.12.4. For pairwise comparisons of means, independent *t*-tests were calculated using the stats package from scipy.

Multiple comparisons of means were performed by ANOVA using the *lm()* function of R after checking that variances were homogeneous across treatments and residuals were close to normality, otherwise specific non-parametric tests were used as specified in the text. Contrasts were addressed using post-hoc Tukey tests. In the case of proportions, we used the *glm()* function with parameter family=*binomial()*. All multiple tests were corrected using Bonferroni procedure.

To quantitatively characterize the distributions of RR among individuals isolated from the evolved populations, symmetry of distributions was tested with the function *symmetry.test()* from the R package "lawstat" with option="MGG" (Miao et al. 2006), side="both", boot=TRUE, B=1000, and q=8/9. The degree of skewness of distributions was quantified using Pearson's third-order moment coefficient of skewness γ_1 (Joanes and Gill 1998).

Results

1. Recombination rate responds to divergent selection

In our divergent selection experiment, we started with an advanced intercross yeast population known as SGRP-4X. SGRP-4X was originally created by recurrently mating four genetically divergent wild founders from the Sake (SA), North America (NA), West African (WA), and Wine/European (WE) clades of *S. cerevisiae*. This highly admixed population results in a representative pool of genetic diversity, which can be used as a powerful tool for mapping quantitative traits (Cubillos et al. 2013).

To artificially select for low- or high-recombination, we bulk-mated SGRP-4X with a tester strain in the SK1 background, which contains two fluorescent markers (VI_C1 and VI_Y2) positioned on chromosome VI (**Suppl Figure S2**). We then recurrently selected for (Sel+) or against (Sel-) spores recombinant within that selection interval VI_C1Y2, based on the segregation of fluorescent signals (**Figure 1**). At each generation of selection, the recombination rate (RR) was phenotyped by sorting non-fluorescent spores obtained from the diploid population, mating back to fluorescent tester haploid strains, and quantifying RR within each interval (**Suppl Figure S2**) on a population level from the segregation of fluorescent signals in spores. It should be noted that because of this selection for non-fluorescent haploids, only RR values measured in even generations are comparable between Sel+, Sel-, and Sel= experiments (see **Figure 1**, fully explained in Materials and Methods).

We performed ten sexual generations of selection in four independent lineages (A, B, C, D) using VI_C1Y2 as the selection interval. When phenotyping RR within this same interval, we observed a clear response to directional selection (**Figure 2A**). The four populations G0, G10 Sel+, G10 Sel=, and G10 Sel- had a significant effect on RR (p-value=2.5×10^{-4}) with all pairwise comparisons significant (p-values<0.016) except G0 *vs* G10 Sel= (p-value=0.998). When looking at the evolution of RR across generations (**Figure 2A**), the curves and their confidence intervals suggest that RR diverged between G0 and G5 or G6. From G6 or G7 on, RR values seem to reach a plateau during which the values of Sel+ and Sel- relative to Sel= were on average +27.6% and -24.5%, respectively.

We observed higher RR values measured in odd than in even generations before G8 (**Figure 2A, B**), consistent with the additional selection applied to odd generations because of our phenotyping method based on sorting non-fluorescent spores (see Materials and Methods).

While RR changes were largely consistent amongst the four biological replicates (**Figure 2B**), one exception can be seen at G5 and G6 for biological replicate C, Sel+. This was expected since there was a failure of the FACS when sorting spores produced by G4 Sel+ C diploids, leading to no selection on recombination. This affected selection both from G4 Sel+ C to G5 Sel+ C but also from G5 Sel+ C to G6 Sel+ C (see **Figure 1A**). As a result, further generations (G7 to G10) of replicate C missed two generations of efficient selection, and thus, replicate C was removed from G5 to G10 in the calculated means (**Figure 2A, C**).

When looking at RRs in the immediately adjacent interval Y2R3 on chromosome VI (**Figure 2C**), RR differed significantly among G0, G10 Sel+, G10 Sel=, and G10 Sel- populations (p-value=3.0×10^{-5}), with all pairwise comparisons significant (p-values<0.011) except G0 *vs* G10 Sel+ (p-value=0.34) and G0 *vs* G10 Sel= (p-value=0.080). However, the responses were in opposite directions as compared to what happened in the VI_C1Y2 interval, where selection was applied. Specifically, when looking at the evolution of RR across generations (**Figure 2C**), the curves and their confidence intervals suggest that between G0 and G4 or G5, RR in Sel+ became lower than in Sel=, and RR in Sel- became higher than in Sel=. In further generations, RR seemed to reach a plateau during which the values of Sel+ and Sel- relative to Sel= were approximately -12% and +13%, respectively. RR data for all individual replicates are available as **Figure 2D**, and do not show any particular difference across biological replicates of a given selection mode.

CO interference estimated *via* the coefficient of coincidence (CoC) did not show any pairwise significant difference among G10 Sel+, G10 Sel-, and G10 Sel= populations (p-values>0.16) in the region including the selected interval (**Suppl Figure S7A, B**) and the immediately adjacent one

(**Suppl Figure S7C, D**).

2. Divergent selection reshapes the distributions of RR values

While the selection process seemed to successfully generate high- and low-recombining populations on average, it was unclear how penetrant these traits were on a population level. Therefore, to gain insights into the distributions of RR values in the evolved populations, we FACS-sorted 1,920 isolated bi-fluorescent diploid cells from generation G8 and phenotyped each of the derived lineages for recombination. Because the FACS cannot distinguish between diploid cells homozygous or hemizygous for the fluorescent markers, only part of these strains were hemizygous, and thus suitable for RR measurement (see Materials and Methods and **Suppl Figure S3**). Among them, we measured RR in 293 Sel+, 101 Sel=, and 376 Sel- strains.

Average RR values for each selection mode were 0.29 for Sel+, 0.26 for Sel=, and 0.19 for Sel- (**Figure 3A**), and these three values were significantly different pairwise (Bonferroni-corrected Wilcoxon rank sum tests, *p*-values<0.00018). Average RR values were not significantly different across biological replicates for Sel= strains (adjusted *p*-value=1). However, in Sel+ strains, average RR values differed significantly (*p*-value=0.047) between replicate C (RR=0.27) and replicates A (RR=0.30), which may be related to the different selection regimes applied to replicate C at generations G5 and G6 (**Suppl Table S3; Suppl Figure S8**).

Figure 3B shows the smoothed distributions of RR values for each of the three selection modes. The Sel= distribution was approximately symmetrical (skewness γ_1=0.144, MGG symmetry test, *p*-value=0.512), whereas the Sel+ distribution was significantly negatively skewed (γ_1= - 0.317, *p*-value<2.2×10^{-16}) and the Sel- distribution was significantly positively skewed (γ_1=0.751, *p*-value<2.2×10^{-16}). The variance of RR in Sel- strains was significantly lower (Fligner-Killeen test) than in Sel= strains (*p*-value=0.0008) and also lower than in Sel+ strains, although less clearly so (*p*-value=0.047). The variance of Sel+ strains showed a tendency to be lower than in Sel= strains, though not significantly (*p*-value=0.052). The overall *shapes* of these distributions were significantly different for all pairs (KS tests, *p*-values<0.00085). This suggests that selection successfully enriched the initial population for individuals carrying high- and low-recombining genotypes.

When isolating bi-fluorescent diploid cells from G8 Sel+ populations, we found two individuals with outlier RR close to 0.5. Such apparent independent segregation of two linked markers may be due to either a drastic increase in RR, or a change in the chromosomal configuration of the fluores-

cent markers, for instance, a translocation or duplication of one marker, or a drastic change in the physical length of the interval between the markers. To investigate these possibilities, we whole-genome sequenced one of these two diploid strains. The results showed that the two markers are still at the prediction positions on chromosome VI and neither of the markers are duplicated at another genomic location (**Suppl Figure S9**). Moreover, Mendelian segregation of both markers confirmed that they are each present at a single locus. Finally, the sequence between the two markers (85 kbp) in the sequenced strain was homozygous and identical to the SK1 sequence, ruling out the idea that some large DNA fragment could have been inserted between the markers. We therefore conclude that the individuals have truly attained a high RR.

3. Selection for high recombination acts on both local (*cis*) and genome-wide (*trans*) levels

Following ten generations of divergent selection, RR responded to selection within the selected interval and in opposite directions in the immediately adjacent one (**Figure 2A, 2C**). However, there appeared to be no differences in RR between Sel+, Sel- and Sel= in other probed regions of chromosomes I and VI (**Suppl Figure S10, Suppl Figure S11**). There was also no significant CoC differences among selection modes at G10 in other probed regions of chromosomes I and VI (**Suppl Figure S7**), but CoC values at G0 were significantly higher than at G10 in both chromosome VI regions (p-value<0.0044).

Collectively, these results suggest that the observed response to selection involved primarily local mechanisms. However, the fluorescent markers used in this phenotyping only probe a very limited proportion of the genome and therefore do not accurately reflect genome-wide recombination patterns, nor do they provide insight into features that may have been selected on the local (*cis*) level.

To gain a more complete view of genome-wide RRs, as well as local (*cis*) factors that may have been selected for, segregants of individual meioses were whole-genome sequenced to quantify recombination rates genome-wide. Given the asymmetric distribution of recombination rates within the Sel+ experiments (see before, and **Figure 3B**), we reasoned that this population may contain lineages with truly high recombination rates as well as some passenger lineages with near wild-type recombination rates. We therefore sequenced the eleven highest-recombining [high] and the eleven lowest-recombining [low] individuals, all isolated from the Sel+ populations at generation G8 (two to three individuals from each biological replicate A, B, C, and D).

Briefly, tetrads from each of the 20 individuals were dissected to acquire four monosporic segregants, which were then sequenced using Illumina short read sequencing. Segregants were sequenced with a minimum read depth of 39X and a mean read depth of 87X (**Suppl Figure S12A**). No chromosomal aneuploidies or large copy number variations were apparent among segregants (visual inspection; **Suppl Figure S13**). Using a custom pipeline (further described in Materials & Methods), the genotype compositions of each segregant were reconstructed. It should be noted that the genotype compositions can only be assigned to one of the four parental genotypes within syntenic regions, so this analysis did not reconstruct genotypes within subtelomeric regions. In addition, the WA and the SK1 tester strain genotypes are so genetically close that they were merged into a single genotype for this analysis.

We first wanted to determine whether there had been any selection for pro-recombinergic features on the local (*cis)* level. Strikingly, the WA and SK1 genotypes were heavily enriched within the Chromosome VI selection interval in [high], but not in [low], segregants (**Figure 4A;** individual tetrads shown in **Suppl Figure S12B)**. This may be because relative to the SK1 tester strain, the parental strain WE has a truncated chromosome VI arm, and the parental strain SA has a deletion within the selection interval (**Suppl Figure S12C**). Together, these results suggest that there has indeed been a selection for pro-recombinergic genotype compositions on the *cis* level. Namely, by enriching for the WA/SK1 genotype within the selection interval of Sel+ populations, the [high] evolved lines have both maximized structural similarity and minimized nucleotide heterozygosity to the SK1 tester strain.

The reconstructed genotypes were next used to determine genome-wide recombination rates. Crossover (CO) events were manually called based on genotype patterns, whereas gene conversion (GC) events were calculated by counting the number of contiguous genome regions containing 3:1 marker patterns (examples shown in **Figure 4B**).

When quantifying the number of recombination events, it should be noted that because there are ‘patches’ where all four chromatids are genetically identical, the precise location or the precise number of COs within these regions cannot be determined, and GCs cannot be detected at all. Therefore, while some COs occurring within these regions can be inferred based on the surrounding genotype pattern, the total CO number will almost always be under-estimated. This is unlikely to confound our analysis, as the number and cumulative size of such genetically identical blocks are very similar between [low] and [high] populations (**Suppl Figure S12D**). [high] samples had a slight but non-significant (*p*-value=0.052) increase in the cumulative size of blocks, meaning that

CO and GC estimates in [high] samples may be more under-represented than in [low] samples, which is conservative. To reduce the impact of these genetically identical patches as a potential confounder, CO and GC rate estimates were adjusted for each sample according to the size and location of the genetically identical patches.

Genome-wide, CO rates, but not GC rates, were significantly higher in [high] individuals than in [low] individuals, regardless of whether variations in the genetically identical patches were adjusted for (**Figure 4C**). Interestingly, different biological replicates seemed to have different genome-wide responses to selection (**Suppl Figure S12E**). Biological replicates A and B showed a more consistent increase in global COs following selection, while biological replicates C and D showed either no response (C) or a milder response (D) to selection. The increase in CO rates was also not uniformly spread through the genome: there were increases (non-adjusted *p*-values<0.05) in chromosomal CO rates on chromosomes III, IX, and IV, slight but non-significant increases on chromosomes II, V, XII and XIII, slight but non-significant decreases in CO rates on chromosomes XI and XIV, and the remaining chromosomes remained unchanged (**Figure 4D**). Surprisingly, there was no apparent increase in the total number of COs on chromosome VI, which contains the selection interval, perhaps due to CO interference. Importantly, the increase in CO rates could be observed on chromosomes besides chromosome VI, suggesting that in addition to selecting for pro-recombinergic *cis* elements, at least some [high] lineages have evolved *trans* effectors increasing CO rate remotely. As we see no concomitant increase in GC rates, we propose that this may be through CO:NCO choice pathways.

4. Single-generation response of RR when relaxing and re-applying selection

Due to a FACS failure, the biological replicate C of Sel+ selection was not properly sorted from G4 to G5, where actually Sel= was applied instead of Sel+. **Figure 2B** shows that RR dropped down to the Sel= level in that replicate C during the single G4 to G5 transition. Proper Sel+ was then applied from G5 to G6, but given the fact that all G4 spores were kept for G5 in the replicate C, the next spore selection from G5 to G6 (i.e., selecting bi-fluorescent and non-fluorescent spores, see **Figure 1A, C**) did not, in fact, particularly select recombinant spores. Thus, as expected, RR in G6 Sel+ C stayed at the same level as in G5 Sel+ C. Selection was efficient at the next generation when sorting from G6 to G7 Sel+ C. Consistently, RR went up from G6 to G7 during that single generation interestingly up to a level higher than in G4.

To try to reproduce such a rapid change in RR and further investigate possible different evolution-

ary trajectories among biological replicates, we took aliquots of the four biological replicates of G8+, and for each of them, we carried out one generation of Sel= followed by one generation of Sel+ (black lines in **Figure 2B**). For replicates A and B, RR did not change much during those two new generations, whereas for replicates C and D, RR values tended to decrease. These replicates C and D thus partially reproduced the rapid drop in RR that was observed in G5 Sel+ C and G6 Sel+ C, although RR values did not reach the level of Sel= populations as in G5 Sel+ C and G6 Sel+ C.

To investigate whether some non-genetic mechanisms might have played a role in the quick responses observed previously when relaxing and re-applying positive selection in replicate Sel+ C, we carried out two generations of Sel+ and Sel= as before, but instead of a genetically diverse G0 population, we started from a diploid SK1 strain without any genetic diversity except the hemizygosity of the two fluorescent markers in the same configuration as in the previous G0. From a strict genetic point of view, no response to selection should be expected then. And in fact, we did not observe any difference between Sel= and Sel+ evolutions for RR, either in the interval selected (**Suppl Figure S14A**), the immediately adjacent interval (**Suppl Figure S14B**), or the other regions on chromosomes I and VI (**Suppl Figure S14D, E, G, H**). Similarly, CoC did not differ between Sel= and Sel+ in all three regions (**Suppl Figure S14C, F, I**).

5. Fitness effects of divergent selection on RR

To investigate possible variations of fitness as an associated response to divergent selection on recombination, we first assessed the extent to which the presence and/or the expression of fluorescent markers may introduce confounding effects on fitness. To do so, we sorted spores from G0 having four different configurations of fluorescent markers [++], [+Y], [C+], and [CY], and measured fitness components on the resulting diploids after panmixis within each category. We observed no significant effect of the fluorescent marker status on growth kinetics parameters maximum rate (*p*-value=0.93; **Suppl Figure S15A**) and plateau (*p*-value=0.56; **Suppl Figure S15B**). However, a significant effect was detected on sporulation rate (*p*-value=0.035) with [+Y] diploids sporulating significantly better than [C+] ones (*p*-value=0.033; **Suppl Figure S15C**), and on spores viability (*p*-value=0.0040) with [+Y] spores being significantly more viable than [C+] ones (*p*-value=0.0021, **Suppl Figure S15D**). Two-factors analysis of variance indicated that the presence of the Y marker insertion had a significant positive effect on spore viability (*p*-value=0,022) and that the presence of the C marker insertion had a significant negative effect (*p*-value=0,0047), but that there was no significant interaction between their effects, so the positive effect of Y might be counteracted by the

negative effect of C in [CY] cells.

Then, to assess the fitness of evolved populations, we sorted non-fluorescent spores from populations G0, G8 Sel+, G8 Sel-, and G8 Sel=, obtained diploids from each category by panmixis, and measured fitness components as before. We observed no significant difference between the four populations for growth kinetics parameters maximum rate and plateau (**Figure 5A, B**), as well as for sporulation rate (**Figure 5C**). However, spore viability in G8 Sel+ and in G8 Sel- were significantly higher than in G8 Sel= and GO populations (**Figure 5D**).

Discussion

The present divergent selection experiment showed a response of local recombination rate after ten generations of direct selection of recombinant or non-recombinant spores in a region of chromosome VI. The experiment was designed to investigate evolutionary mechanisms during a limited number of generations. The response to selection is thus most likely due to selection and recombination among allelic variants present in the starting population, rather than accumulated novel mutations. To further limit the occurrence of mutations, we kept the number of mitotic cell divisions low (approximately 10 mitotic cycles per sexual generation). On the other hand, to maximize the standing genetic variation, four of the five founder parents used to build the initial SGRP-4X population were chosen to capture as much as possible of the genetic diversity of the *S. cerevisiae* species (Cubillos et al. 2013). Moreover, the genomic interval chosen for selecting recombinant spores was previously found to show a high level of variation in recombination rate across these five founders (Raffoux et al. 2018a). Indeed, we observed a plateau in the response to selection after about eight generations (**Figure 2A**), suggesting that we've reached the limits allowed by the initial genetic variation and thus that the impact of novel mutations on that response was probably limited.

The experimental protocol used in this work was designed to sort 300,000 cells at each generation. The main bottleneck in our experiments is due to FACS, so population size should never be less than 300,000 throughout all steps of all sexual generations. Genetic differentiation between G0 and Sel= populations is thus expected to be mainly due to unwanted selection (e.g. on growth, sporulation, viability) rather than genetic drift. Therefore, using Sel= populations as a control should allow us to investigate the effect of selection on recombination without confounding effects of drift or unwanted selection on other traits.

We do not know of any similar experiment performed previously in *S. cerevisiae*. In *S. pombe*, an experiment of evolution under selection for recombinant or non-recombinant spores was reported in a recent PhD dissertation (Berenguer Millanes 2025). The author carried out a similar approach based on FACS-sorting spores expressing fluorescent proteins, but the initial diploid was obtained by crossing two quasi-isogenic variants (differing only at a few marker loci) from a single Leupold lab strain, so the main source of genetic variance allowing for evolution was novel mutation. After 36 meiotic generations, the author observed a significant positive response when selecting double-recombinant spores in two adjacent intervals on Chromosome I, but unclear results in single intervals. It should be noted that (1) in such selection for double recombinants, the effective selection pressure applied on RR is much stronger than in our case (single interval) because it requires two different COs, and (2) the absence of crossover interference in *S. pombe* also makes simultaneous selection on two close intervals more effective than in *S. cerevisiae*. More generally, quantitative genetics studies within and between species suggest that RR is expected to display a weak response to short-term selection (Payseur 2025). Our results are consistent with previous works showing that RR is able to evolve under selective pressure, e.g., in Drosophila (Detlefsen and Roberts 1921; Chinnici 1971a; Chinnici 1971b; Charlesworth and Charlesworth 1985a) and other species, see large review in (Stapley et al. 2017).

In our experiment, selection was stronger in Sel+ than in Sel- since spores selected in Sel- may result from hidden recombination between the markers (**Figure 1A**). Quantitatively, the expected frequency of spores produced with a (hidden) recombination event between the marker loci, among all spores kept by the FACS in Sel- regime, ranges between zero and 1/3 as RR ranges between 0 and 0.5, so one could expect selection to be more efficient in Sel+. However, we observed no clear difference in the absolute values of slopes of the responses between Sel+ and Sel- (**Figure 2A**).

We observed an inverted response to divergent selection in the interval next to the one where selection was applied. This may be due to CO interference: if local determinants drive double-strand breaks to be preferentially repaired into COs in one region, then interference is expected to commit double-strand breaks surrounding that region to the NCO pathway, thus depleting COs in adjacent intervals. When we assessed the strength of interference along generations, no significant changes were observed between Sel+, Sel-, and Sel= experiments, indicating that changes in interference strength were not the main mechanism that led to modified CO frequency as a response to selection. In the interval VI_R3Y4C5, we measured surprisingly high values of CoC (greater than one in the first three generations) whereas CoC values became stable and lower than 1 in further generations.

Values of CoC greater than one are supposed to indicate negative interference, which is not in accordance with our previous measurements of positive interference (corresponding to gamma parameter nu>1) with the same method in the founder strains of the SGRP-4x population (Raffoux et al. 2018a). Given the high variance associated with the data, we suggest that negative interference measured in generations G0 to G2 should be taken with care. Nevertheless, in other regions too, we observed a similar tendency of interference to increase (*i.e.*, of CoC to decrease) across generations, whatever the mode of selection, Sel+, Sel-, or Sel=. If this increase is related to genetic changes in the population, it cannot be due to our selection on recombination, but might be a consequence of unwanted selection on some other traits, which is unavoidable in experimental evolution, particularly when sporulation is involved in the selection cycle.

Phenotyping individuals isolated from the evolved populations revealed that eight generations of directional selection reduced the variance of RR values in the selected interval for Sel+ and Sel- experiments, but not in the Sel= control. This may be explained by the fact that strong selection generally reduces genetic diversity, which in turn results in reduced phenotypic variance. Still, in both Sel+ and Sel- evolved populations, we observed continuous distributions of RR (**Figure 3B**) with gradual changes in the mean across generations as compared to Sel= (**Figure 2A**), pointing to the fact that we've successfully evolved population-level changes in the recombination rates, without only selecting for some strong recombination variant. However, the shapes of the distributions were also modified, with a negatively skewed distribution in G8 Sel+ and a positively skewed distribution in G8 Sel-, while the distribution remained symmetrical in G8 Sel= (**Figure 3B**). These two asymmetric distributions might be explained by considering the hypothesis of a rather strong QTL affecting RR. The Sel+ population would mainly contain individuals carrying the 'high RR' allele at this QTL, visualized by the highest peak on the right side of the red curve in **Figure 3B**, and a minority of individuals with the 'low RR' allele revealed by the shoulder on the left side of the red curve. Symmetrically, the Sel- population would mainly contain individuals carrying the 'low RR' allele at this QTL, visualized by the highest peak on the left side of the blue curve in **Figure 3B**, and a minority of individuals with the 'high RR' allele revealed by the shoulder on the right side of the blue curve. In Sel=, both alleles would have similar frequencies, which would result in the observed symmetrical distribution. Moreover, the Sel= curve shows three peaks, and the shapes of Sel+ and Sel- curves also suggest a possible third bump between the two main parts of the peaks, which might correspond to the three genotypes of a codominant QTL. Elsewhere, in Sel-, the peak is higher than in Sel+, indicating a greater loss of variance. This may suggest that selection was

stronger in Sel- than in Sel+ experiments, which is not expected given our experimental design allowing some hidden recombinants to be selected in Sel-. Another hypothesis is that higher recombination in Sel+ increased the genetic variance by creating new allele combinations, thus reducing the loss of variance due to selection.

Following selection within the chromosome VI_C1Y2 interval, the responses in RR in the five other intervals carrying fluorescent markers suggest a *cis*-only change in RR. However, the regions probed by fluorescent markers are very limited as compared to the whole genome, leading us to sequence individual [high] and [low] segregants from G8 Sel+ to obtain a genome-wide and higher-resolution picture of recombination landscapes. [high] samples almost universally showed an increase in homozygosity to the chromosome VI SK1 tester strain (both for sequence and at the structural level), suggesting a strong selection on the *cis* level, which is in accordance with previous observations in *S. cerevisiae* (Raffoux et al. 2018a). In addition, we observed a significantly higher genome-wide CO number in [high] compared to [low] tetrads. Given that COs are relatively rare on a per-chromosome level, the data are noisy and statistical power is low, but we also observed a (non-significant) trend to increase on chromosomes not containing the selection interval. Together, these suggest an addition selection on the *trans* level.

Intriguingly, the tetrads sequenced from the four G8 Sel+ evolution lines (*i.e.*, biological replicates A, B, C, and D) appeared to increase the chromosome VI recombination rates through different mechanisms that we were able to discern by sequencing individual segregants from each tetrad: In tetrads from G8 Sel+ A [high] and G8 Sel+ B [high], we observed consistently high genome-wide recombination rates (80, 89, 81, 87, and 87 COs per tetrad), suggesting successful selection for genome-wide increases in recombination rates, as intended. Conversely, in G8 Sel+ C [high] and G8 Sel+ D [high], we did not observe high genome-wide recombination rates (68, 69, 73 COs per tetrad), and we observed no striking abnormalities on the *cis* level. It is therefore unclear why the tetrads sequenced from G8 Sel+ C [high] and G8 Sel+ D [high] display high recombination rates within the chromosome VI selection interval. These different behaviors between replicates A and B on one side, and C and D on the other side may be related to the RR changes observed when we relaxed selection for two generations in the four G8 Sel+ biological replicates (black lines in **Figure 2B**). Such variation in evolutionary outcomes of technically identical experimental setups highlights the power of this approach for uncovering biological novelty.

In the biological replicate C of Sel+ experiment (**Figure 2B**), when the selection pressure was relaxed (all spores were kept instead of only recombinant ones) between G4 and G5, RR went back to

its initial level within only one generation, and recovered its G4 value as soon as recombinant spores were again specifically selected, which occurred only at G7 (see Results, and **Figure 1A**). When we tried to reproduce the same situation by relaxing spore selection starting from each of the four biological replicates of the G8 Sel+ population, a similar response was observed for replicates A and B, but replicates C and D were not affected by the change in the selection mode (black lines in **Figure 2B**). These results raise the question of which kind of genetic element or factor affecting recombination could have its frequency massively altered in a single generation without selection, and massively recovered in a single generation when selecting again recombinant spores. Because the action of this element was observed at the local level only, one could think of a sequence motif with major local effect, such as a hotspot, and/or a particular diploid genotype with an inhibitory effect on COs, due, for instance, to heterozygosity of a structural variant such as an inversion or a deletion. Although we have not identified the real mechanism at work in our experiment, it seems to be able to play an important role in the response to directional selection.

Our results show that eight generations of divergent selection on recombination did not change growth kinetics (**Figure 5A, B**) or sporulation rate (**Figure 5C**). Given the experimental design involving mitotic growth and sporulation steps, it is likely that some unwanted selective pressure was applied on these traits, so an increase of fitness may have been expected between G0 and G8 generations. However, the SGRP-4X population had already undergone 12 generations of sexual reproduction before we started our experiments (Cubillos et al. 2013), so major alleles controlling these fitness components may have already been more or less fixed. On the other hand, spore viability in G8 Sel+ and in G8 Sel- were significantly higher than in G8 Sel= and GO populations (**Figure 5D**). Because it increased CO rates to some extent genome-wide, the Sel+ treatment may have reduced the frequency of achiasmatic bivalents leading to aneuploidy, thus increasing the ability of spores to germinate as compared to the Sel= case. However, this does not explain why Sel- populations also gained better spore viability than Sel= ones. A hypothesis might be that this is due to fitness effects of the fluorescent markers inserted in the genome. Indeed, [C+] spores were less viable — but [+Y] spores more viable — than [++] spores (**Suppl Figure S15**), both effects being more or less additive (see Results). The advantage of being [+Y] might be explained by the fact that severely non-viable spores, which could not express fluorescent proteins, cannot be present in the [+Y] class but may be present in the [++] class, introducing some sampling bias. Besides that, [C+] spores might be less viable than [++] ones because of some deleterious effect of C marker insertion: even though we checked that the insertions did not disrupt any known coding sequence, it might alter some fit-

ness-related regulatory element. Altogether, the gain in viability of Sel- spores as compared to Sel= spores may not be clearly attributed to confounding effects of the fluorescent markers.

In conclusion, the recurrent divergent selection approach used in this work proved to be an efficient way to investigate the ability of the recombination rate to respond to directional selection. A clear response was observed rather symmetrically in both directions in the selected region. *Cis* effects were observed at the sequence level, but *trans* effects were also detected, providing quite direct evidence that various types of recombination modifiers are at work to control the evolution of recombination through multiple paths. It also suggests that the ones at work in our experiments involve some QTLs with quite strong effects contributing to the response.

Data availability statement

Yeast strains produced in this work are available upon reasonable request. All data underlying this article will be publicly available in the french government data warehouse 'Recherche Data Gouv' (https://recherche.data.gouv.fr/en) under the persistent DOI: https://doi.org/10.57745/YTFYTT. A provisional confidential access is possible for reviewing purposes at: https://moulon.inrae.fr/DATA_GENETICS-2026-309198/ (User name: GENETICS, Password: ahd6yuVu). R and Python codes used to analyze the data and produce graphs and conclusions are publicly available in the french government software forge 'ForgeMIA' at https://forge.inrae.fr/gqe-base/evolrec_wp1.

Acknowledgements

The authors thank Mickael Bourge for many years of sharing with us his invaluable experience in cytometry analysis, Mickaël De Carvalho for having so many discussions with us about the project, and Domenica Manicacci for helpful comments on the manuscript and advice on statistical analyses.

Study funding

The present work has benefited from Imagerie-Gif core facility supported by I'Agence Nationale

de la Recherche (FBI ANR-24-INBS-0005 (BIOGEN); SPS ANR-17-EUR-0007, EUR SPS-GSR) and with financial support from ITMO Cancer of Aviesan and INCa on funds administered by Inserm. This work has also benefited from funding from the EVOLREC (ANR-20-CE13-0010) and CO-PATT (ANR-20-CE12-0006) projects. GQE—Le Moulon benefits from the support of the LabEx Saclay Plant Sciences-SPS (ANR-10-LABX-0040-SPS).

Conflict of interest

The authors declare no conflict of interest

Figure Legends

Figure 1. Details of the three modes of selection applied to spores. In Sel+ experiments, only recombinant spores are selected by FACS-sorting **(A)**, in Sel-, only non-recombinant spores are selected by FACS-sorting **(B)**, and in Sel= controls, all spores are kept **(C)**. Note that in Sel+, two selection cycles are represented on the sketch: odd generations on the top side of the circle, and even generations on the bottom side of the circle. In contrast, for Sel- and Sel=, one single cycle of selection is represented in the sketch.

Figure 2. Response of recombination to divergent selection. Recombination rate in the interval VI_C1Y2, where selection was applied **(A, B)** and in the adjacent interval VI_Y2R3 **(C, D)**. Left panels **(A, C)**: averages and 95% confidence intervals of RR based on four biological replicates. Right panels **(B, D)**: values of each individual replicate (named with colored letters A, B, C, and D on the plots). Black triangles represent the mean of four technical replicates (black circles) of phenotyping the G0 population. Dashed red lines indicate odd generations of Sel+ experiments. Red, green, and blue solid lines indicate Sel+ (even generations), Sel=, and Sel- experiments, respectively. Black lines in panels **B** and **D** correspond to aliquots of generation G8 Sel+ which were submitted to one generation of relaxed selection as for Sel=, and then again to the Sel+ regime. The chromosome sketch on the left side of the figure indicates the positions of the two intervals considered on chromosome VI.

Figure 3. Recombination rate of individuals isolated from G8 populations. Individual values of recombination rate in the selected interval VI_C1Y2 **(A)** and their smoothed distributions **(B)** measured from 323 Sel+, 377 Sel-, and 101 Sel= isolated diploid individuals from populations at gener-

ation G8, after pooling biological replicates A, B, C, D. Dashed lines indicate the means of distributions.

Figure 4. Genome-wide analysis of recombination at G8. (A): Meta-analysis across chrVI of parental allele frequency in segregants derived from 9 highest-recombining ([high]) tetrads and 11 lowest-recombining tetrads ([low]) at generation G8 of Sel+ selection. The selection interval used for recombination phenotyping, as well as tetrad selection, is indicated in grey. **(B):** Examples of crossover (CO) and gene conversion (GC) calling in a [high] and [low] tetrad. Given the presence of genetically identical patches within each tetrad, both COs and GCs are under-represented, and precise locations cannot always be determined. **(C):** Genome-wide quantification of COs and GCs in [low] and [high] segregants, both with and without adjusting for genetically identical patches. **(D):** CO quantification by chromosome, with chromosomes ordered by increasing size. *p*-value indicates the non-adjusted result of each independent *t*-test.

Figure 5. Effect of selection for recombination on fitness. Maximum growth rate **(A)**, concentration at the plateau **(B),** sporulation rate **(C)**, and spore viability **(D)** of populations at generation G8 for Sel+, Sel=, and Sel- selection modes, and of the initial population G0. The four biological replicates were pooled. Boxplots were made from a minimum of 30 independent measurements for A and B, and of 6 (C) or 8 (D) independent countings of 96 spores. Pairwise statistical comparisons shown on the graph correspond to Bonferroni-adjusted *p*-values. * <0.05, ** <0.01, *** <0.001.

Supplementary Figure Legends

Figure S1. Procedure used to build the population G0 from the SGRP-4X population. Mixed spores from SGRP-4X (Mat-a or Mat-α ho::hygMX ura3::kanMX, lys2::URA3 or LYS2) were mated with a fluorescent SK1-VI_C1Y2 tester (Mat-a ho::hygMX ura3::kanMX VI-C1:TDH3prom-yECerulean-NatMX VI-Y2:TDH3prom-Venus-NatMX). Diploids hemizygous for the fluorescent markers were then selected based on their ability to grow on medium without Uracil containing nourseothricin.

Figure S2. Marker positions in the testers used to probe recombination rate. These testers are SK1 strains containing three fluorescent markers, used to cross to non-fluorescent cells to measure recombination rate in six different intervals: two on chromosome I and four on chromosome VI

(among which the VI_C1Y2 interval where selection was applied). C, Y, R refer to markers yECerulean, Venus, and mRFP, respectively.

Figure S3. Phenotyping recombination rate of individuals isolated from G8 populations. Experimental design and expected diploid frequencies after FACS-sorting bi-fluorescent diploid cells in the case of Sel+ and Sel- (upper panel) or Sel= (lower panel) experiments.

Figure S4. Distribution of fluorescent marker frequency in spores from individuals isolated from G8 populations. (A): Marker yECerulean. **(B):** Marker Venus. X-axis: marker frequency. Y-axis: number of isolated individuals. Red lines: lower and upper boundaries defined as median +/- 3 times Median Absolute Deviation. Green dashed lines correspond to a frequency value of 0.5.

Figure S5. Distribution of haplotype frequency ratios in spores from individuals isolated from G8 populations. X-axis: haplotype frequency ratios $F_{[CY]}/\left(F_{[CY]}+F_{[++]}\right)$ **(A)** and $F_{[C+]}/\left(F_{[C+]}+F_{[+Y]}\right)$ **(B)**. Y-axis: number of isolated individuals. Red lines: lower and upper boundaries defined as median +/- 3 times Median Absolute Deviation.

Figure S6. Distribution of haplotype frequency ratios in spores from individuals isolated from G8 populations for each selection mode. X-axis: selection mode: Sel+ (red), Sel= (green), and Sel- (blue). Y-axis: haplotype frequency ratios $F_{[CY]}/\left(F_{[CY]}+F_{[++]}\right)$ **(A)** and $F_{[C+]}/\left(F_{[C+]}+F_{[+Y]}\right)$ **(B)**. Red dashed lines: lower and upper boundaries defined as median +/- 3 times Median Absolute Deviation.

Figure S7. Crossover interference across generations of selection. Coefficient of coincidence (CoC) based on two adjacent intervals delimited by three fluorescent markers, in two regions of chromosome VI **(A, B, C, D)**, and in one region of chromosome I **(E, F)**. CoC=1 corresponds to no interference, whereas CoC<1 corresponds to positive interference. **(A, C, E):** Mean CoC values and 95% confidence intervals based on four biological replicates. **(B, D, F):** CoC values of each individual biological replicate. Dashed red lines indicate even generations of Sel+ experiments. Red, green, and blue solid lines indicate Sel+ (odd generations), Sel=, and Sel- experiments, respectively. The chromosome sketches on the left side of the figure indicate the positions of the pairs of intervals considered.

Figure S8. **Recombination rates of individuals isolated from G8 populations per selection mode and per replicate.** Individual values of recombination rate in the selected interval VI_C1Y2 for each biological replicate A, B, C, D, and each selection mode Sel+ (red), Sel= (green), and Sel- (blue).

Figure S9. **ChrVI sequence analysis of an outlier hyper-recombinant strain.** Alignment against the region of the SK1 chromosome VI reference sequence (bottom) between the fluorescent markers used for selection. All sequences above the reference are 16 ONT long reads obtained from a strain having an outlier recombination rate equal to 0.491. This strain was isolated from the G8 Sel+ population. Grey color indicates a match with the reference sequence (including shared gaps), red color indicates mismatches, and black color indicates gaps.

Figure S10. Response to selection in two other genomic regions on chromosome VI. Recombination rate in the two regions VI_R3Y4 **(A, B)** and VI_Y4C5 **(C, D)**. **(A, C):** Means and 95% confidence intervals based on four biological replicates (named with colored letters A, B, C, and D on the plots). **(B, D):** Individual values of each biological replicate. Dashed red lines indicate even generations of Sel+ experiments. Red, green, and blue solid lines indicate Sel+ (odd generations), Sel=, and Sel- experiments, respectively. Black lines in panels **B** and **D** correspond to aliquots of generation G8 Sel+ which were submitted to one generation of relaxed selection as for Sel=, and then again to the Sel+ regime. The chromosome sketch on the left side of the figure indicates the positions of the two intervals considered on chromosome VI.

Figure S11. Response to selection in two genomic regions on chromosome I. Same as Figure S10 but in two regions of chromosome I: I_R2C3 **(A, B)** and I_C3Y4 **(C, D)**.

Figure S12 Genome-wide analysis of recombination following eight generations of selection. (A): Mean read depth for each of the 80 sequenced sergregants. **(B):** Individual genotype compositions across chromosome VI for the 9 high-recombining ([high]) tetrads and 11 low-recombining tetrads ([low]) at G8 Sel+. **(C)**: Homology plot for chromosome VI between the 4 parental genotypes (SA, NA, WA, WE) as well as the SK1 tester strain. Each grey connection bar represents a section of homology detected by mVISTA (probability threshold 0.5) with an additional filter of minimum conservation 85% and minimum block size 1 kbp. **(D):** Quantification of the number (left) and cumulative size (right) of the four-way genetically identical patches in which GCs cannot be detected, and COs cannot be precisely located. **(E):** Breakdown of the CO rate shown in Figure 4C by biological replicate. *p*-value indicates the non-adjusted result of each independent *t*-test.

Figure S13 CNV analysis of all sequenced segregants. Genome-wide read counts of 80 sequenced segregants to ensure that there are no chromosomal aneuploidies or major CNVs. Each data point represents an average read count across a non-overlapping 5-kbp window.

Figure S14. Response to selection without initial genetic diversity. Recombination rate (RR) and coefficient of coincidence (CoC) during two generations of selection for recombinant spores (Sel+,

red lines) or without selection (Sel=, green lines) from a SK1 VI_C1Y2 diploid strain hemizygous for the two fluorescent markers C (yECerulean) and Y (Venus) on chromosome VI. Values of RR at each generation in intervals VI_C1Y2 where selection was applied **(A),** VI_Y2R3 **(B)**, VI_R3Y4 **(D)**, and VI_Y4C5 **(E)** of chromosome VI, and I_R2C3 **(G)** and I_C3Y4 **(H)** of chromosome I, and coefficients of coincidence (CoC) in double intervals VI_C1Y2R3 **(C)** and VI_R3Y4C5 **(F)** of chromosome VI, and I_R2C3Y4 **(I)** of chromosome I.

Figure S15. Effect of fluorescent markers on growth kinetics. Maximum growth rate **(A)**, concentration at the plateau **(B)**, sporulation rate **(C)**, and spore viability **(D)** of sub-samples (N>50,000) of population G0 sorted according to the presence of fluorescent markers. X-axis: ++, +Y, C+, and CY indicate the presence of fluorescent markers: no marker, Venus only, yECerulean only, and yECerulean and Venus, respectively. Boxplots were made from a minimum of 110 independent measurements for (**A**) and (**B**), and of 4 (**C**) or 8 (**D**) independent countings of 96 spores. Pairwise statistical comparisons shown on the graph correspond to Bonferroni-adjusted *p*-values. * <0.05, ** <0.01.

Supplementary Tables

Table S1. Details of all fluorescent marker constructions inserted in the genome of the testers

Table S2. Selection of diploid strains isolated from G8 Sel+ populations for tetrad sequencing

Table S3. Effect of selection mode and biological replicate on RR measured in 770 individuals isolated from the populations at generation G8. Bonferroni-adjusted *p*-values from pairwise Wilcoxon Test.

REFERENCES

Abdullah, Borts RH. 2001. Meiotic recombination frequencies are affected by nutritional states in Saccharomyces cerevisiae. PNAS. 98(25):14524–14529. https://doi.org/10.1073/pnas.201529598

Abdullah, Charlesworth B. 1974. Selection for reduced crossing over in Drosophila melanogaster. Genetics. 76(3):447–451. https://doi.org/10.1093/genetics/76.3.447

Aggarwal DD et al. 2015. Experimental evolution of recombination and crossover interference in Drosophila caused by directional selection for stress-related traits. BMC Biol. 13(1):101. https://doi.org/10.1186/s12915-015-0206-5

Allard RW. 1963. Evidence for Genetic Restriction of Recombination in the Lima Bean. Genetics. 48(10):1389–1395

Anderson LK et al. 2003. High-Resolution Crossover Maps for Each Bivalent of Zea mays Using Recombination Nodules. Genetics. 165(2):849–865

Anderson LK, Reeves a, Webb LM, Ashley T. 1999. Distribution of crossing over on mouse synaptonemal complexes using immunofluorescent localization of MLH1 protein. Genetics. 151(4):1569–79

Barton NH. 2010. Mutation and the evolution of recombination. Philosophical Transactions of the Royal Society B: Biological Sciences. 365(1544):1281–1294. https://doi.org/10.1098/rstb.2009.0320

Bauer E et al. 2013. Intraspecific variation of recombination rate in maize. Genome Biology. 14(9):R103. https://doi.org/10.1186/gb-2013-14-9-r103

Bell G. 1982. The Masterpiece of Nature: The Evolution and Genetics of Sexuality. Routledge, UK.

Berenguer Millanes C. 2025. The recombination landscape of fission yeast: Natural variation and the effects of direct selection and inversions on the evolution of recombination. Fakultät für Biologie, Ludwig-Maximilians-Universität München. https://edoc.ub.uni-muenchen.de/35321/6/Berenguer_Millanes_Cristina.pdf

Blary A, Jenczewski E. 2019. Manipulation of crossover frequency and distribution for plant breeding. Theor Appl Genet. 132(3):575–592. https://doi.org/10.1007/s00122-018-3240-1

Brekke C, Johnston SE, Gjuvsland AB, Berg P. 2023. Variation and genetic control of individual recombination rates in Norwegian Red dairy cattle. Journal of Dairy Science. 106(2):1130–1141. https://doi.org/10.3168/jds.2022-22368

Burt A, Bell G. 1987. Mammalian chiasma frequencies as a test of two theories of recombination. Nature. 326(6115):803–805. https://doi.org/10.1038/326803a0

Camacho C et al. 2009. BLAST+: architecture and applications. BMC Bioinformatics. 10:421. https://doi.org/10.1186/1471-2105-10-421

Charlesworth B. 1993. The Evolution of Sex and Recombination in a Varying Environment. J Hered. 84(5):345–350. https://doi.org/10.1093/oxfordjournals.jhered.a111355

Charlesworth B, Barton NH. 1996. Recombination load associated with selection for increased recombination. Genetics Research. 67(1):27–41. https://doi.org/10.1017/S0016672300033450

Charlesworth B, Charlesworth D. 1985a. Genetic variation in recombination in Drosophila . I. Responses to selection and preliminary genetic analysis. Heredity. 54(1):71–83. https://doi.org/10.1038/hdy.1985.10

Charlesworth B, Charlesworth D. 1985b. Genetic variation in recombination in Drosophila. II. Genetic analysis of a high recombination stock. Heredity. 54(1):85–98

Chelysheva L et al. 2012. The Arabidopsis HEI10 Is a New ZMM Protein Related to Zip3. PLOS Genetics. 8(7):e1002799. https://doi.org/10.1371/journal.pgen.1002799

Chinnici JP. 1971a. Modification of Recombination Frequency in Drosophila. I. Selection for Increased and Decreased Crossing over. Genetics. 69(1):71–83

Chinnici JP. 1971b. Modification of Recombination Frequency in Drosophila. II. the Polygenic Control of Crossing over. Genetics. 69(1):85–96

Cubillos FA et al. 2013. High-Resolution Mapping of Complex Traits with a Four-Parent Advanced Intercross Yeast Population. Genetics. 195(3):1141–1155. https://doi.org/10.1534/genetics.113.155515

Denis E et al. 2018. Extracting high molecular weight genomic DNA from Saccharomyces cerevisiae. [accessed 2026 Feb 23]. https://www.protocols.io/view/extracting-high-molecular-weight-genomic-dna-from-4r3l29jw4v1y/v1. https://doi.org/10.1038/protex.2018.076

Detlefsen JA, Roberts E. 1921. Studies on crossing over. I. The effect of selection on crossover values. Journal of Experimental Zoology. 32(2):333–354. https://doi.org/10.1002/jez.1400320206

Dewees AA. 1975. Genetic modification of recombination rate in Tribolium castaneum. Genetics. 81(3):537–552. https://doi.org/10.1093/genetics/81.3.537

Dluzewska J, Szymanska M, Ziolkowski PA. 2018. Where to Cross Over? Defining Crossover Sites in Plants. Front Genet. 9 [accessed 2020 Mar 20]. https://www.frontiersin.org/articles/10.3389/fgene.2018.00609/full. https://doi.org/10.3389/fgene.2018.00609

Ebinuma H, Yoshitake N. 1981. The Genetic System Controlling Recombination In The Silkworm. Genetics. 99(2):231–245. https://doi.org/10.1093/genetics/99.2.231

Falque M et al. 2009. Two Types of Meiotic Crossovers Coexist in Maize. The Plant Cell. 21(12):3915–3925. https://doi.org/10.1105/tpc.109.071514

Falque M et al. 2024. MiniRead: A simple and inexpensive do-it-yourself device for multiple analyses of micro-organism growth kinetics. Yeast. 41(5):307–314. https://doi.org/10.1002/yea.3932

Fernandes JB et al. 2017. Unleashing meiotic crossovers in hybrid plants. PNAS. 201713078. https://doi.org/10.1073/pnas.1713078114

Gandon S, Otto SP. 2007. The Evolution of Sex and Recombination in Response to Abiotic or Coevolutionary Fluctuations in Epistasis. Genetics. 175(4):1835–1853. https://doi.org/10.1534/genetics.106.066399

Goddard MR, Godfray HCJ, Burt A. 2005. Sex increases the efficacy of natural selection in experimental yeast populations. Nature. 434(7033):636–640. https://doi.org/10.1038/nature03405

Gowen JW. 1919. A Biometrical Study of Crossing Over. on the Mechanism of Crossing over in the Third Chromosome of DROSOPHILA MELANOGASTER. Genetics. 4(3):205–250

Haenel Q, Laurentino TG, Roesti M, Berner D. 2018. Meta-analysis of chromosome-scale crossover rate variation in eukaryotes and its significance to evolutionary genomics. Molecular Ecology. 27(11):2477–2497. https://doi.org/10.1111/mec.14699

Higgins JD, Armstrong SJ, Franklin CH, Jones GJ. 2004. The Arabidopsis MutS homolog AtMSH4 functions at an early step in recombination: evidence for two classes of recombination in Arabidopsis. Genes and Development. 18:2557–2570

Hill WG, Robertson A. 1966. The effect of linkage on limits to artificial selection. Genetics Research. 8(3):269–294. https://doi.org/10.1017/S0016672300010156

Housworth EA, Stahl FW. 2003. Crossover Interference in Humans. The American Journal of Human Genetics. 73(1):188–197. https://doi.org/10.1086/376610

Hunter N, Chambers SR, Louis EJ, Borts RH. 1996. The mismatch repair system contributes to meiotic sterility in an interspecific yeast hybrid. The EMBO Journal. 15(7):1726–1733. https://doi.org/10.1002/j.1460-2075.1996.tb00518.x

Joanes DN, Gill CA. 1998. Comparing measures of sample skewness and kurtosis. Journal of the Royal Statistical Society: Series D (The Statistician). 47(1):183–189. https://doi.org/10.1111/1467-9884.00122

Johnston SE. 2024. Understanding the Genetic Basis of Variation in Meiotic Recombination: Past, Present, and Future. Molecular Biology and Evolution. 41(7):msae112. https://doi.org/10.1093/molbev/msae112

Jones A et al. 2021. High-molecular weight DNA extraction, clean-up and size selection for long-read sequencing. PLoS One. 16(7):e0253830. https://doi.org/10.1371/journal.pone.0253830

Jones GH. 1984. The control of chiasma distribution. Symp Soc Exp Biol. 38:293–320

Kidwell MG. 1972. Genetic Change in Recombination Value In Drosophila Melanogaster. I. Artificial Seleciton For High And Low Recombination And Some Properties Of Recombination-Modifying Genes. Genetics. 70(3):419–432. https://doi.org/10.1093/genetics/70.3.419

Kong A et al. 2010. Fine-scale recombination rate differences between sexes, populations and individuals. Nature. 467(7319):1099–1103. https://doi.org/10.1038/nature09525

Korol AB, Iliadi KG. 1994. Increased recombination frequencies resulting from directional selection for geotaxis in Drosophila. Heredity (Edinb). 72 (Pt 1):64–68. https://doi.org/10.1038/hdy.1994.7

Liu H et al. 2017. Direct Determination of the Mutation Rate in the Bumblebee Reveals Evidence for Weak Recombination-Associated Mutation and an Approximate Rate Constancy in Insects. Molecular Biology and Evolution. 34(1):119–130. https://doi.org/10.1093/molbev/msw226

Lloyd A, Morgan C, Franklin C, Bomblies K. 2018. Plasticity of Meiotic Recombination Rates in Response to Temperature in Arabidopsis. Genetics. genetics.300588.2017. https://doi.org/10.1534/genetics.117.300588

Long A, Liti G, Luptak A, Tenaillon O. 2015. Elucidating the molecular architecture of adaptation

via evolve and resequence experiments. Nature Reviews Genetics. 16(10):567–582. https://doi.org/10.1038/nrg3937

Mancera E et al. 2008. High-resolution mapping of meiotic crossovers and non-crossovers in yeast. Nature. 454(7203):479–85. https://doi.org/10.1038/nature07135

Martini E, Diaz RL, Hunter N, Keeney S. 2006. Crossover Homeostasis in Yeast Meiosis. Cell. 126(2):285–295. https://doi.org/10.1016/j.cell.2006.05.044

McDonald MJ, Rice DP, Desai MM. 2016. Sex speeds adaptation by altering the dynamics of molecular evolution. Nature. 531(7593):233–236. https://doi.org/10.1038/nature17143

Miao W, Gel YR, Gastwirth JL. 2006. A new test of symmetry about an unknown median. In: Random Walk, Sequential Analysis and Related Topics. WORLD SCIENTIFIC; p 199–214 [accessed 2026 Feb 12]. https://www.worldscientific.com/doi/abs/10.1142/9789812772558_0013. https://doi.org/10.1142/9789812772558_0013

Morgan C, Howard M, Henderson IR. 2024. HEI10 coarsening, chromatin and sequence polymorphism shape the plant meiotic recombination landscape. Current Opinion in Plant Biology. 81:102570. https://doi.org/10.1016/j.pbi.2024.102570

Novak TE et al. 2026. Caloric density alters meiotic recombination rate in Drosophila melanogaster. Genetica. 154(1):7. https://doi.org/10.1007/s10709-025-00255-2

Otto SP, Lenormand T. 2002. Resolving the paradox of sex and recombination. Nat Rev Genet. 3(4):252–261. https://doi.org/10.1038/nrg761

Otto SP, Payseur BA. 2019. Crossover Interference: Shedding Light on the Evolution of Recombination. Annual Review of Genetics. 53(1):19–44. https://doi.org/10.1146/annurev-genet-040119-093957

Pan J et al. 2011. A hierarchical combination of factors shapes the genome-wide topography of yeast meiotic recombination initiation. Cell. 144(5):719–31. https://doi.org/10.1016/j.cell.2011.02.009

Pan Q, Deng M, Yan J, Li L. 2017. Complexity of genetic mechanisms conferring nonuniformity of recombination in maize. Sci Rep. 7 [accessed 2017 Nov 6]. https://www.ncbi.nlm.nih.gov/pmc/articles/PMC5430679/. https://doi.org/10.1038/s41598-017-01240-2

Parée T, Teotónio H. 2025. Experimental tests on the evolution of sex and recombination and their adaptive significance. j evol Biol. 38(7):798–810. https://doi.org/10.1093/jeb/voaf028

Parsons PA. 1958. Selection for Increased Recombination in Drosophila melanogaster. The American Naturalist. 92(865):255–256. https://doi.org/10.1086/282033

Payseur BA. 2025. Genetics of recombination rate variation within and between species. j evol Biol. 38(7):851–860. https://doi.org/10.1093/jeb/voae158

Petit M et al. 2017. Variation in Recombination Rate and Its Genetic Determinism in Sheep Populations. Genetics. 207(2):767–784. https://doi.org/10.1534/genetics.117.300123

Raffoux X et al. 2018a. Role of Cis, Trans, and Inbreeding Effects on Meiotic Recombination in Saccharomyces cerevisiae. Genetics. 210(4):1213–1226.

https://doi.org/10.1534/genetics.118.301644

Raffoux X et al. 2018b. High-throughput measurement of recombination rates and genetic interference in Saccharomyces cerevisiae. Yeast. 35(6):431–442. https://doi.org/10.1002/yea.3315

Raffoux X, Falque M. 2024. CAYSS: Package for Automatic Cytometry Analysis of Yeast Spore Segregation. Yeast. 41(11–12):681–690. https://doi.org/10.1002/yea.3988

Rockmill B, Lambie EJ, Roeder GS. 1991. [9] Spore enrichment. In: Methods in Enzymology. Vol. 194. Academic Press; p 146–149 (Guide to Yeast Genetics and Molecular Biology). [accessed 2024 Sept 18]. https://www.sciencedirect.com/science/article/pii/0076687991940122. https://doi.org/10.1016/0076-6879(91)94012-2

Sardell JM, Kirkpatrick M. 2020. Sex Differences in the Recombination Landscape. The American Naturalist. 195(2):361–379. https://doi.org/10.1086/704943

Shaw DD. 1972. Genetic and environmental components of chiasma control. Chromosoma. 37(3):297–308. https://doi.org/10.1007/BF00319872

Stapley J et al. 2017. Variation in recombination frequency and distribution across eukaryotes: patterns and processes. Philos Trans R Soc Lond B Biol Sci. 372(1736):20160455. https://doi.org/10.1098/rstb.2016.0455

Sturtevant AH. 1915. The behavior of the chromosomes as studied through linkage. Molecular and General Genetics MGG. 13(1):234–287. https://doi.org/10.1007/BF01792906

Tourrette E, Bernardo R, Falque M, Martin OC. 2019. Assessing by Modeling the Consequences of Increased Recombination in Recurrent Selection of Oryza sativa and Brassica rapa. G3: Genes, Genomes, Genetics. g3.400545.2019. https://doi.org/10.1534/g3.119.400545

Ziolkowski PA et al. 2017. Natural variation and dosage of the HEI10 meiotic E3 ligase control Arabidopsis crossover recombination. Genes Dev. 31(3):306–317. https://doi.org/10.1101/gad.295501.116

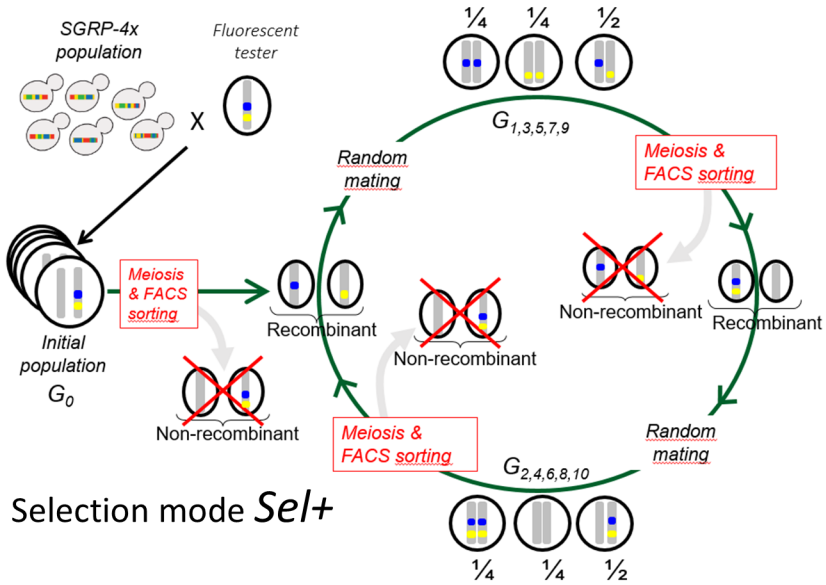

A Selection mode *Sel+*

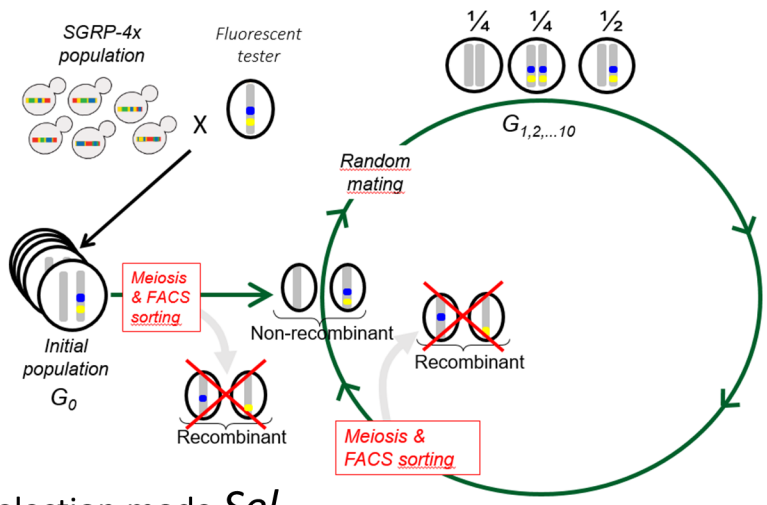

B Selection mode *Sel-*

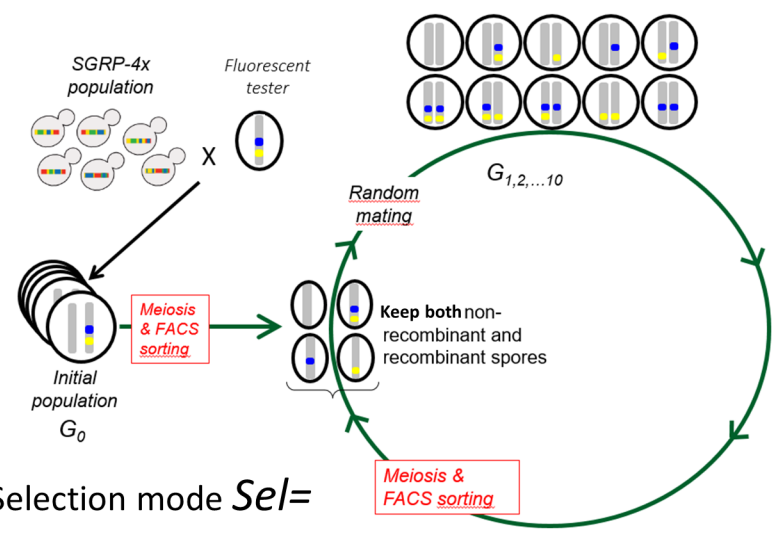

C Selection mode *Sel=*

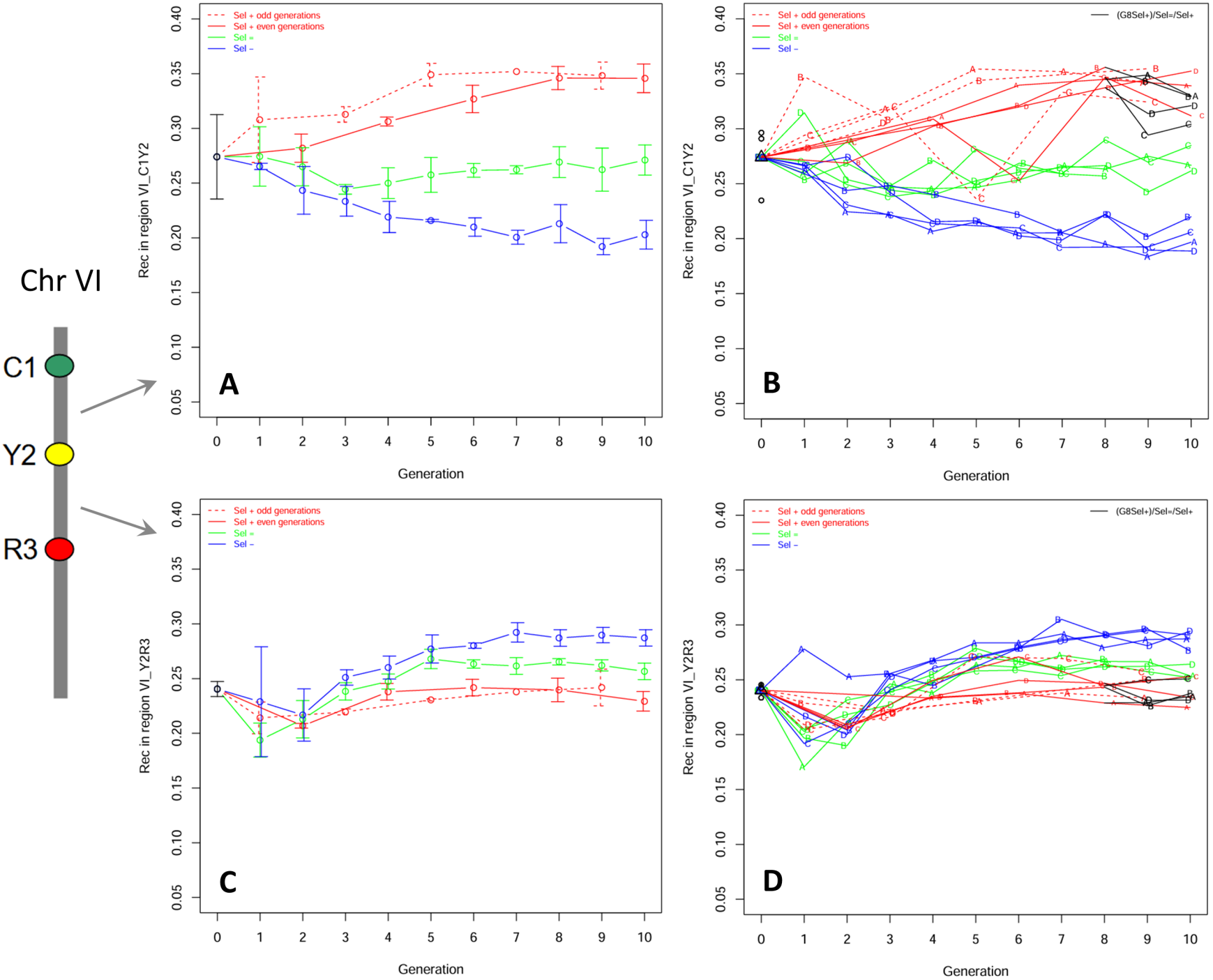
Chr VI
C1
Y2
R3
Sel + odd generations
Sel + even generations
Sel =
Sel –
(G8Sel+)/Sel=/Sel+
Rec in region VI_C1Y2
Rec in region VI_Y2R3
Generation
A
B
C
D

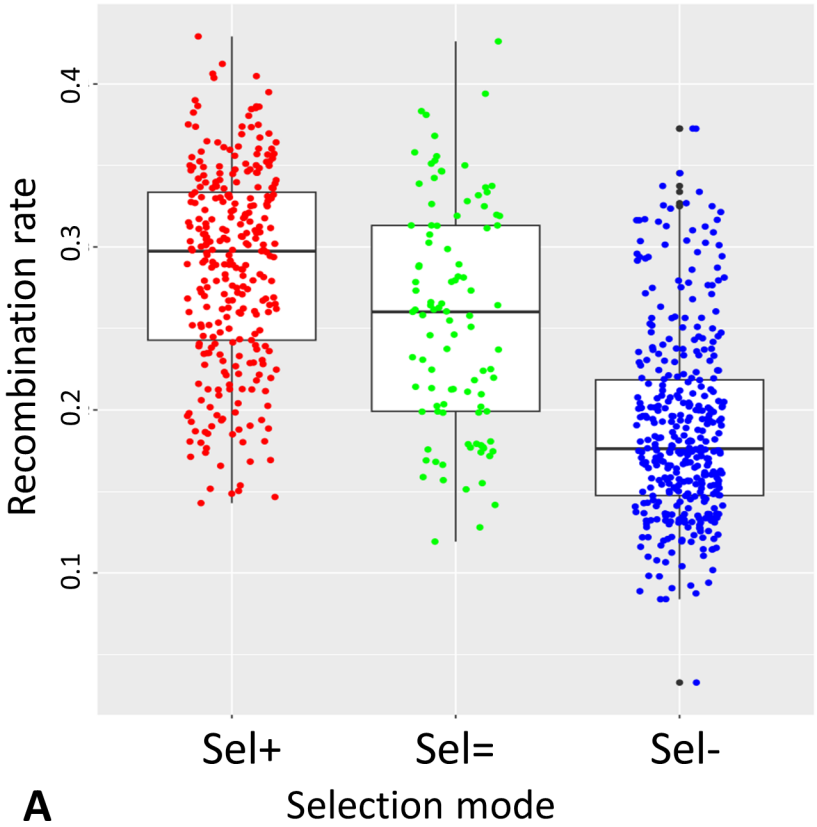
Recombination rate
0.1
0.2
0.3
0.4
Sel+
Sel=
Sel-
Selection mode
A

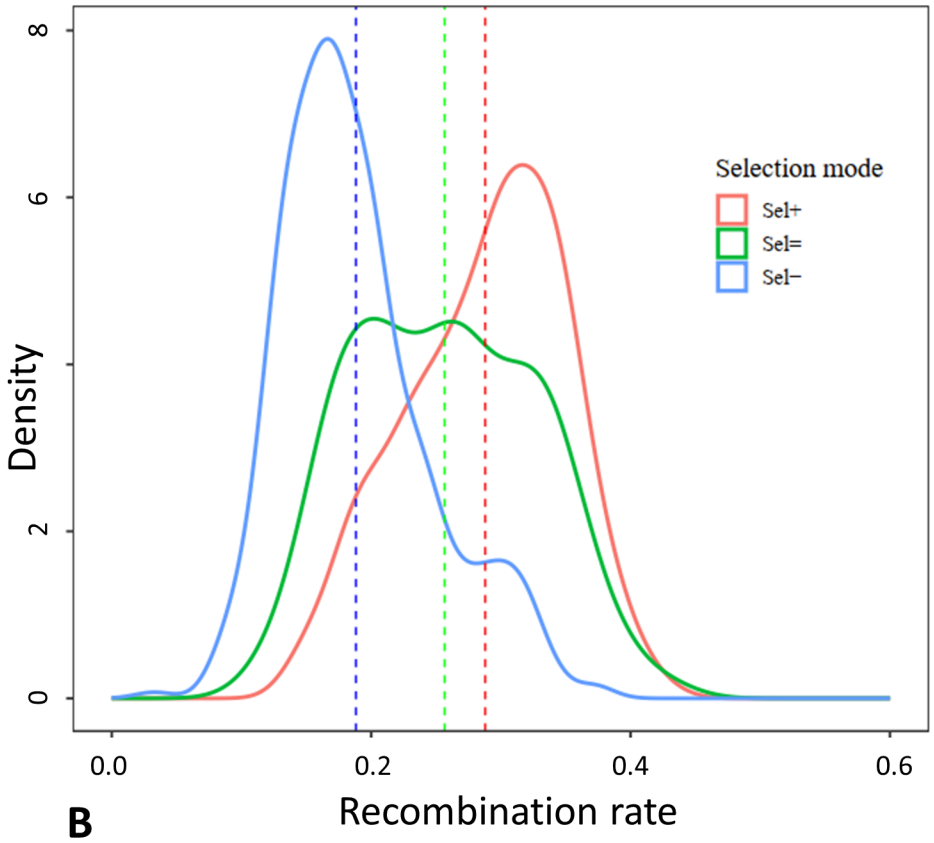
Density
0
2
6
8
0.0
0.2
0.4
0.6
Recombination rate
Selection mode
Sel+
Sel=
Sel−
B

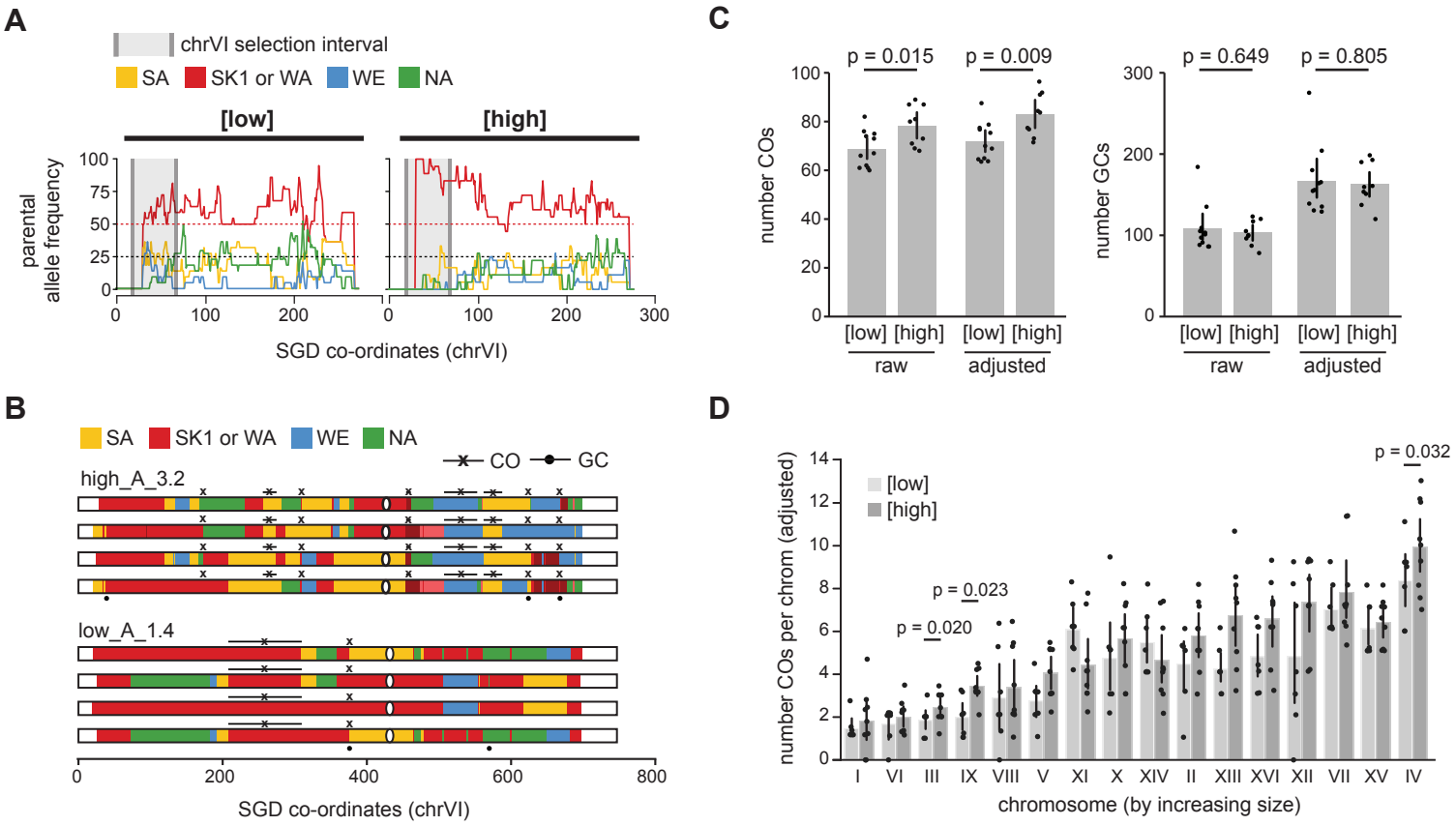
A
chrVI selection interval
SA
SK1 or WA
WE
NA
[low]
[high]
parental allele frequency
SGD co-ordinates (chrVI)
B
SA
SK1 or WA
WE
NA
CO
GC
high_A_3.2
low_A_1.4
SGD co-ordinates (chrVI)
C
p = 0.015
p = 0.009
p = 0.649
p = 0.805
number COs
number GCs
[low] [high]
raw
adjusted
D
[low]
[high]
p = 0.032
p = 0.023
p = 0.020
number COs per chrom (adjusted)
I VI III IX VIII V XI X XIV II XIII XVI XII VII XV IV
chromosome (by increasing size)

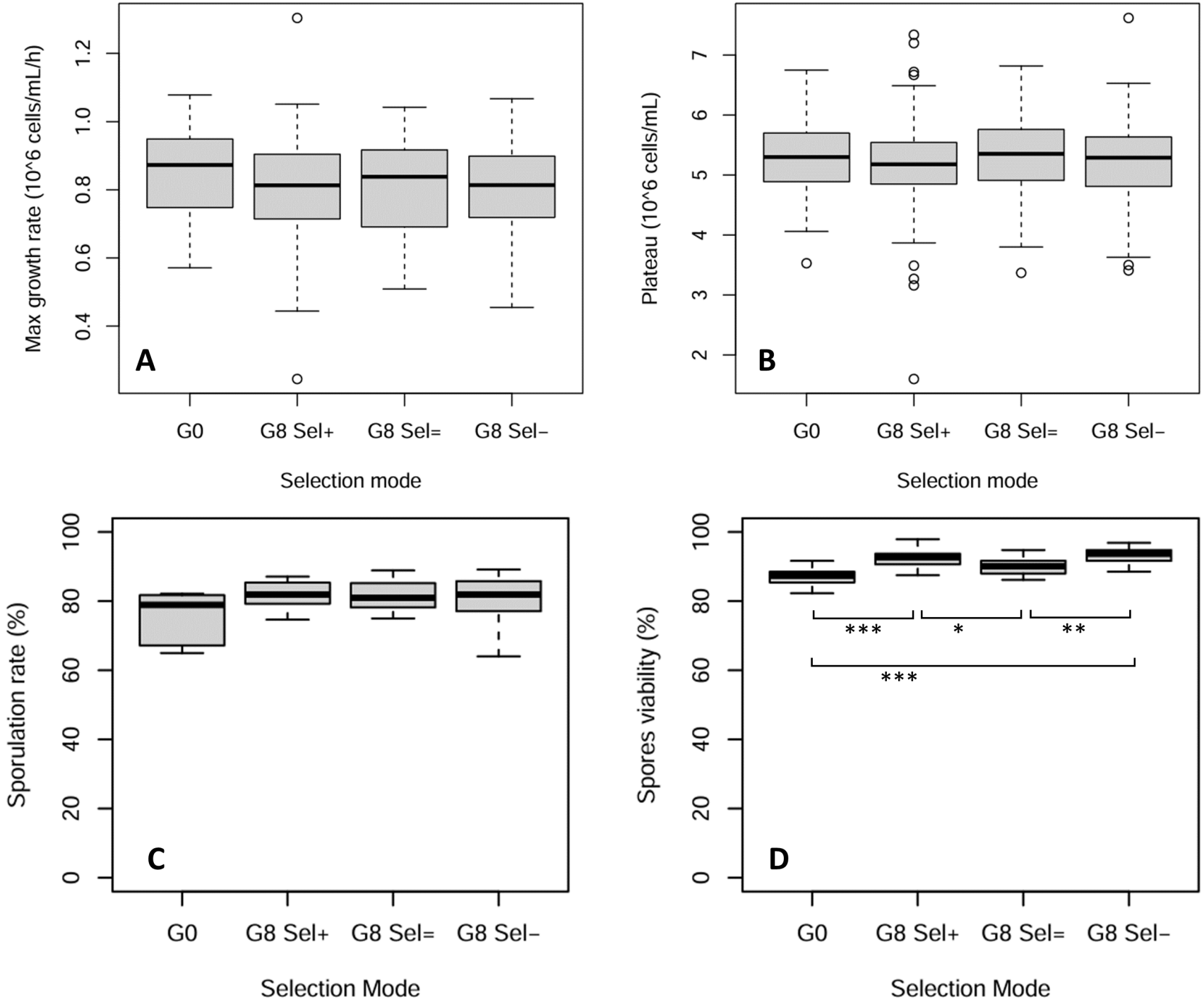
A
Max growth rate (10^6 cells/mL/h)
0.4
0.6
0.8
1.0
1.2
G0
G8 Sel+
G8 Sel=
G8 Sel−
Selection mode
B
Plateau (10^6 cells/mL)
2
3
4
5
6
7
G0
G8 Sel+
G8 Sel=
G8 Sel−
Selection mode
C
Sporulation rate (%)
0
20
40
60
80
100
G0
G8 Sel+
G8 Sel=
G8 Sel−
Selection Mode
D
Spores viability (%)
0
20
40
60
80
100
***
*
**
***
G0
G8 Sel+
G8 Sel=
G8 Sel−
Selection Mode